

INTERNATIONAL ULTRAVIOLET EXPLORER

CAMERA USERS' GUIDE

(IUE Technical Note 31)

C Coleman\*  
E Golton  
P Gondhalekar  
J Hall  
M Oliver  
M Sandford  
T Snijders\*  
B Stewart

(\*editors)

Issue	Date
1	October 1977

UNIVERSITY COLLEGE LONDON

APPLETON LABORATORY

## IUE CAMERA USERS' GUIDE

Issue 1 of the IUE Camera Users' Guide has been written by members of the UK Camera Operations Group and edited by C Coleman and T Snijders. In order to make sure that this issue is available for the Science Operations Training Course to be held at GSFC 24 October - 4 November 1977, there has been insufficient time to subject it to the usual project review, and it is known to the authors to contain several inaccuracies and deficiencies. I request that any comments, criticisms, suggestions or contributions are sent to me by 14 November 1977. We propose that a fully reviewed and approved issue 2 be made just before launch and that issue should be available to the guest observers to assist them in preparations for their observations. The relation between this Guide and the overall IUE Users' Guide still needs to be defined.

M C W Sandford  
Chairman, UK Camera Operations Group

## Distribution for Tech. Note 31, issue 1.

UK	US	ESA
B Anderson	A Boggess	P Benvenuti
P Barker	F Carr	J Faelker
C Coleman	D Evans	F Macchetto
E Dunford	C Fuechsel	
E Golton	D KlingleSmith	
P Gondhalekar	G Longanecker	
J Hall	D West	
M Oliver	C Wu	
M Sandford		
T Snijders		
B Stewart		
D Stickland		
P Vaughan		
K Ward		
R Wilson		
A Boksenberg		
V Harrison		

+ 24 Copies for Science Operations Course Attendees not included above.

Contents

	<u>Page</u>
1. INTRODUCTION	1-1
2. THE IUE SPECTROGRAPH CAMERAS	2-1
2.1 The Ultraviolet-to-Visible Image Converter	2-2
2.2 The SEC Television Camera Tube	2-4
2.3 Electronics	2-8
2.4 Camera Operating Sequences	2-10
2.4.1 STANDBY mode	2-10
2.4.2 EXPOSE mode	2-10
2.4.3 READ mode	2-11
2.4.4 PREPARE sequence	2-11
2.5 References	2-12
3. CAMERA PERFORMANCE	3-1
3.1 Sensitivity	3-1
3.1.1 Quantum efficiency	3-1
3.1.2 Photoelectron sensitivity and intensity transfer function	3-3
3.2 Signal-to-Noise Ratio and Dynamic Range	3-7
3.3 Resolution	3-14
3.3.1 The central core of the point spread function	3-14
3.3.2 Halation	3-15
3.3.3 Astronomical implications	3-16
3.4 Geometrical Distortion	3-22
3.5 Background	3-23
3.5.1 Dark emission from the UVC and SEC photocathodes	3-23
3.5.2 Particle radiation	3-23
3.5.3 Random bright spots	3-24
3.5.4 UVC phosphorescence	3-24
3.6 Over-Exposure	3-27
3.6.1 Camera safety	3-27
3.6.2 Data integrity	3-27

3.7	Image Imperfections	3-28
3.8	References	3-29
4.	OPTIMUM USE OF CAMERAS	4-1
4.1	Available Options	4-2
4.2	Discussion of Options	4-3
4.2.1	Epoch of observation and scheduling	4-3
4.2.2	Spectrograph	4-4
4.2.3	Entrance aperture and dispersion	4-4
4.2.4	Camera	4-4
4.2.5	PREPARE sequence	4-5
4.2.6	SEC camera tube gain	4-5
4.2.7	Exposure time	4-6
4.2.8	Head-amplifier gain	4-8
4.2.9	Pixel size, scan format and telemetry rate	4-8
4.3	Classes of Observation and Setting of Operational Parameters	4-9
4.4	Calibration Images	4-11
5.	IMAGE PROCESSING SOFTWARE	5-1
5.1	IUE Spectral Image Processing System (IUESIPS)	5-3
5.2	Removal of Telemetry Errors	5-4
5.3	Periodic Noise Removal	5-5
5.4	Geometric Correction	5-6
5.5	Photometric Correction (ITF Correction)	5-7
5.6	Background Removal	5-8
5.7	Correction for Image Imperfections	5-9
5.8	Resolution Enhancement	5-10
5.9	Wavelength Determination	5-11
5.10	Extraction of Spectra from Corrected Images	5-12
5.11	Order Overlap and Scattered Light Correction	5-13
5.12	Sky Background Removal	5-14
5.13	System Sensitivity Correction	5-15
5.14	References	5-16
6.	GROUND STATION DISPLAY FACILITIES	6-1
6.1	Image Display	6-1
6.1.1	The IUE Experiment Display System (EDS)	6-1
6.1.2	Photowrite	6-1
6.2	Camera Operational Display	(6-1)
	Appendix A: List of Abbreviations and Acronyms	A-1

## List of Figures

<u>Figure No.</u>		<u>Page</u>
1-1	Optical schematic of the IUE Scientific Instrument	1-3
1-2	IUE spectral formats	1-4
2.1-1	The ultraviolet-to-visible image converter	2-3
2.2-1	The SEC television camera tube	2-6
2.2-2	Image display format, showing pixel addressing convention and fiducial mark positions	2-7
2.3-1	IUE camera sub-system electronics	2-9
3.1-1	Typical spectral response for the IUE cameras	3-2
3.1-2	Intensity transfer function for SWP camera	3-5
3.1-3	Contour map of sensitivity variations across the image area	3-6
3.2-1	Signal-to-noise ratio as a function of camera gain and exposure level	3-10
3.2-2	Variation of signal-to-noise ratio over the image area	3-11
3.2-3	Signal-to-noise ratio as a function of exposure level at SEC MAXG for all cameras	3-12
3.2-4	Signal-to-noise ratio as a function of exposure level at SEC MEDG for all cameras	3-13
3.3-1	Camera point spread and modulation transfer functions	3-17
3.3-2	Dependence of resolution on wavelength	3-18
3.3-3	Variation of resolution over the image area	3-19
3.3-4	Variation of halation over the image area (254 nm)	3-20
3.3-5	Variation of halation over the image area (122 nm)	3-21
3.5-1	Radiation-induced background as a function of orbital position	3-26
5-1	IUE Spectral Image Processing System (IUESIPS)	5-2

The IUE experiment is designed to obtain high-resolution ultraviolet spectra of astronomical objects down to a faint limit of  $\sim 15^m$ . The satellite, which is in an eccentric geosynchronous orbit, is in communication with the European ground-station (VILSPA, Madrid) for about twelve hours per day and with the US ground-station continuously.

The scientific instrument (SI) on board the satellite consists of a three-axis-stabilised 45 cm f/15 telescope feeding two high-resolution echelle spectrographs which together cover the spectral range 115-320 nm at a resolution of  $\sim 10^{-2}$  nm; an alternative low-dispersion mode (resolution  $\sim 0.6$  nm, with correspondingly higher sensitivity) is available, and may be selected by ground command. Each spectrograph contains a prime and a redundant (back-up) camera. The spectrograph optics and the Fine Error Sensors (FES - used for stellar acquisition and guidance) are shown schematically in Fig. 1-1 and are described in detail elsewhere in the IUE Users' Guide (§00.00); the most important characteristics of the SI optics are summarised in Table 1-1, and the spectral formats for both high- and low-dispersion modes are illustrated in Fig. 1-2.

The remainder of this section of the IUE Users' Guide is concerned particularly with the spectrograph cameras. Their construction, operation and performance are discussed in sufficient detail to enable the guest astronomer to plan his observations most efficiently and to make the best use of the resulting observational data. To this end, the software image correction procedures and ground-station display facilities are described in the last two chapters of this section. Engineering details, operational procedures and constraints are documented in the Camera Operations Manual (IUE Technical Note 30). Further information on any of the topics discussed below may be obtained from references cited in the text and from documents such as the IUE System Design Report and the manuals for the various sub-systems.

Table 1-1

Optical Characteristics of the IUE Scientific Instrument

1. Telescope

Configuration:	Ritchey-Chrétien
Primary mirror diameter:	45 cms
Effective focal ratio:	f/15
Central obscuration:	50% (linear diameter)
Image scale at focal plane:	30.5 arc-sec/mm (32.7 $\mu$ m/arc-sec)
FES acquisition field:	16 arc-min diameter
Guidance capability:	<u>+0.5 arc-sec</u>

2. Long-Wavelength Spectrograph

Entrance apertures:	(i) 3 arc-sec diameter circular (not shuttered) (ii) 10 x 20 (arc-sec) <sup>2</sup> elliptical
Spectral range:	180-320 nm
Resolving power:	(i) High-dispersion mode: $1.5 \times 10^4$ (ii) Low-dispersion mode: 250
Dispersion at cameras:	(i) High-dispersion mode: 0.125-0.197 nm/mm (ii) Low-dispersion mode: $\sim 6$ nm/mm
Optical efficiency (telescope + spectrograph):	4.2% at 254 nm 0.45% at 200 nm

3. Short-Wavelength Spectrograph

Entrance apertures:	(i) 3 arc-sec diameter circular (not shuttered) (ii) 10 x 20 (arc-sec) <sup>2</sup> elliptical
Spectral range:	115-190 nm
Resolving power:	(i) High-dispersion mode: $1 \times 10^4$ (ii) Low-dispersion mode: 167
Dispersion at cameras:	(i) High-dispersion mode: 0.086-0.137 nm/mm (ii) Low-dispersion mode: $\sim 6$ nm/mm
Optical efficiency:	(telescope + spectrograph): 2.2% at 191nm 1.7% at 122nm

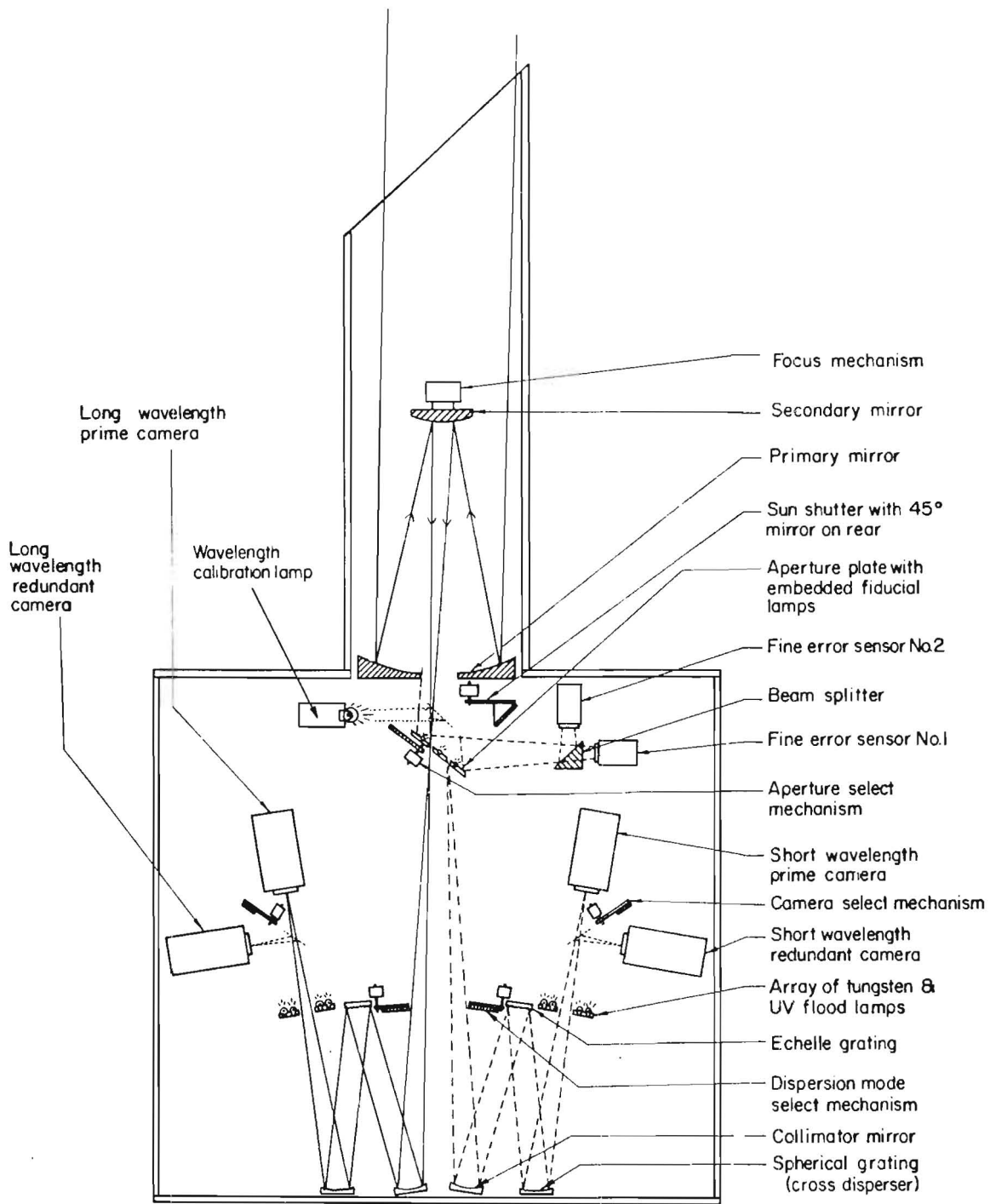


Fig. 1-1 Optical schematic of the IUE Scientific Instrument.



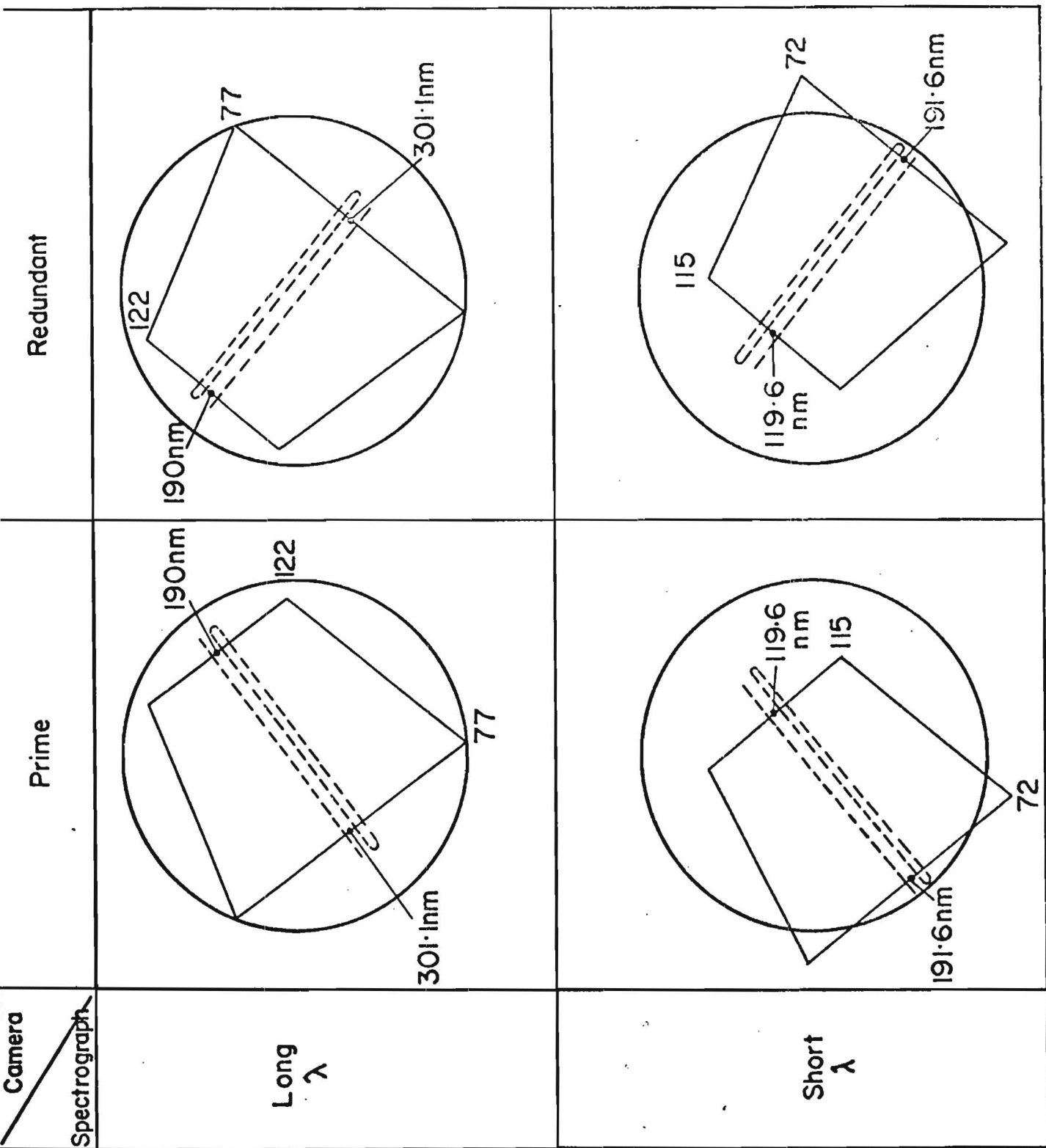


Fig. 1-2

IUE spectral formats for prime and redundant long and short wavelength cameras. The circles define the 25 mm diameter active area of the camera. Wavelengths are marked at the centre of the extreme echelle orders (order numbers are given at the corners of the trapezia which outline the extent of the free spectral range). Positions of the low-dispersion spectra obtained using the small and large apertures are shown by the broken lines.

## 2. THE IUE SPECTROGRAPH CAMERAS

The IUE television camera systems convert two-dimensional spectra from the spectrographs into video signals suitable for transmission to the ground stations. The cameras for long and short wavelength spectrographs are of identical construction, although certain minor differences in performance exist between them. Each camera sub-system is comprised of four modules. The Camera Head Module (CHM) contains the electro-optical detector components and some of the electronics such as the video head-amplifier which must be in close proximity to the television camera tube. The remaining three modules supply the rest of the camera electronic functions; these are briefly described in §2.3 below. The basic detector tube in the CHM is a SEC television camera; as this is sensitive only to visible light, it is preceded by an ultraviolet-to-visible image converter. These components are described in the following sections; further information on electro-optical low-light-level image detectors may be found in Ref. 2-1.

## 2.1 The Ultraviolet-to-Visible Image Converter (UVC)

The UVC (ITT, type F4122) is a 40 mm diameter proximity-focused tube (Fig. 2.1-1). It has a magnesium fluoride entrance window (transparent down to  $\sim 115$  nm) on which is deposited a semi-transparent caesium telluride photocathode; this is highly efficient (10-20%) in the ultraviolet but relatively insensitive to visible light (§3.1.1). The photocathode converts the incident ultraviolet spectrum into a corresponding photoelectron image; these photoelectrons are accelerated by a high electric field (5 kV across a 1.3 mm gap) and proximity-focused onto the output phosphor screen where much of their energy is dissipated in the production of photons of blue light (the yield at the phosphor is typically 60 photons out per photoelectron, and with a photocathode efficiency of  $\sim 15\%$  the overall gain of the UVC is  $\sim 10$  blue photons out per ultraviolet photon in). The efficiency of the screen is maximised by a surface layer of aluminium which reflects backward-emitted photons in the direction of the output window; this also eliminates optical feedback. A matt black coating over the aluminium layer minimises halation effects due to ultraviolet photons transmitted by the photocathode and reflected back to it.

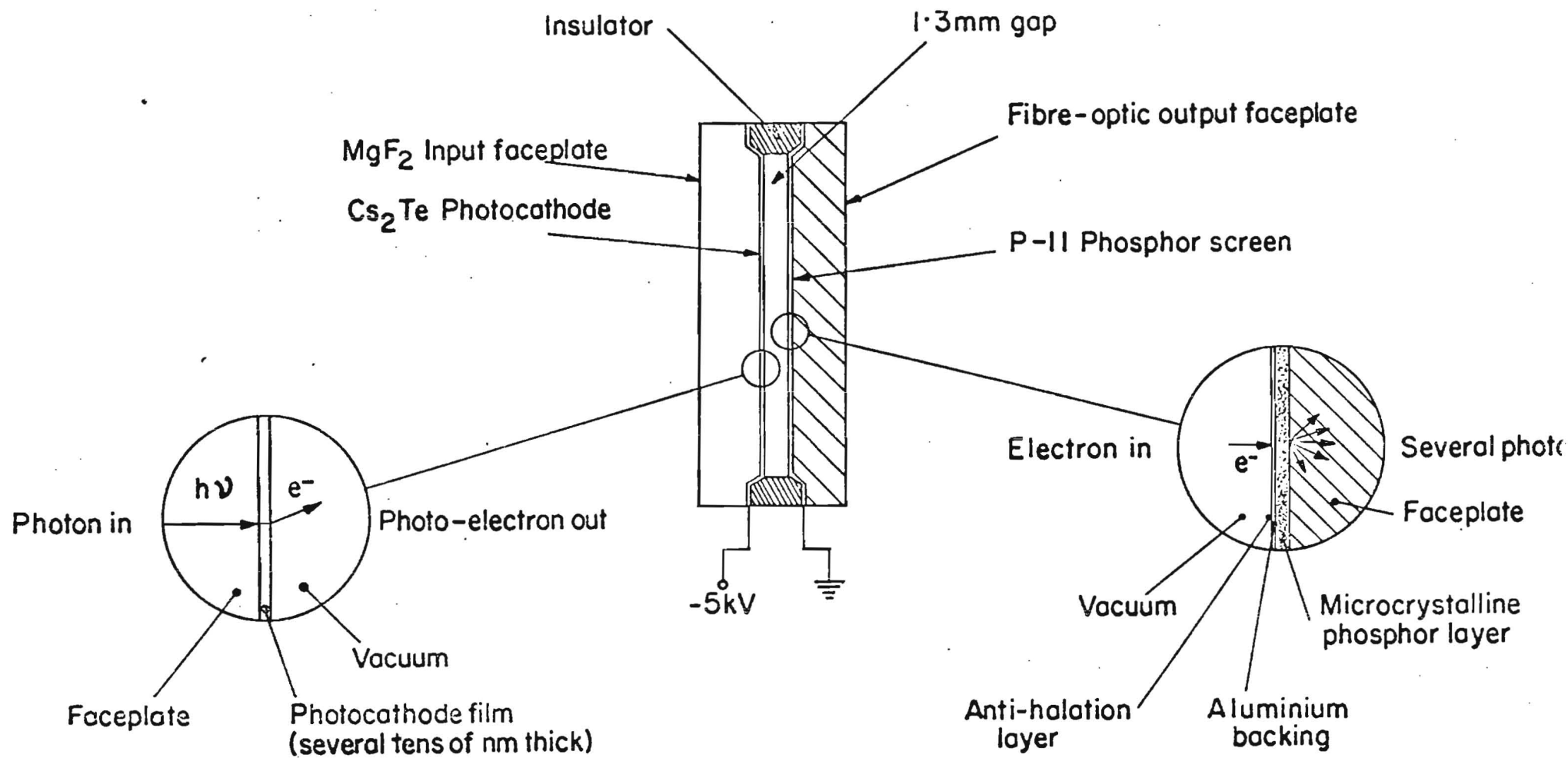


Fig. 2.1-1 Schematic diagram of the ultraviolet-to-visible image converter.

## 2.2 The SEC Television Camera Tube (Fig. 2.2-1)

The converted image from the UVC is transferred via a fibre-optic coupling to the blue-sensitive bialkali photocathode of the SEC tube. Included in this fibre-optic coupling is a set of fiducial marks - a square array of 13 x 13 opaque areas each 100  $\mu\text{m}$  square and  $(2.0 \pm 0.005)$  mm apart - which provides a geometrical reference for the evaluation of the spectra (Fig. 2.2-2).

The photoelectron image generated at the SEC tube's photocathode is accelerated through the electrostatically-focused image section onto the target. The target (Ref. 2-2) consists of a low-density porous layer of potassium chloride ( $\sim 10\mu\text{m}$  thick) supported by an aluminium oxide membrane ( $\sim 50\text{nm}$  thick) and backed by a thin aluminium signal plate. Some fraction of the energy of each photoelectron is expended in the production of several secondary electrons in the potassium chloride; these are swept towards the signal plate by a 12V bias across the target (this process is termed Secondary Electron Conduction - SEC) leaving a multiplied positive charge image on the target. The secondary electron gain (positive charges on target per incident photoelectron) is a function of the incident electron energy; at the highest voltage setting "MAXG" ( $\sim 6.1$  kV) the gain is  $\sim 50$  whilst at the lower settings "MEDG" ( $\sim 4$  kV) and "MING" ( $\sim 3.2$  kV) the gain is reduced to  $\sim 15$  and  $\sim 5$  respectively. The gain process in the SEC target is initially linear but has a saturating characteristic (§3.1.2). Because of the highly insulating nature of the target, an image may be integrated and stored for many hours; there is no detectable reciprocity failure.

The readout section of the camera tube is similar to that of a standard magnetically-focused vidicon, although its operation is somewhat different in that the beam is deflected digitally to scan a raster of 768 x 768 pixels (picture elements) in 37 $\mu\text{m}$  steps across the image.\* At each pixel, the

---

\*In the VICAR image-processing system (§5), pixel positions are referred to by their "line" and "sample" numbers. As viewed on any of the display systems, line 1 (the first line to be read out) is at the top of the picture and line 768 is at the bottom. Along each line, the sample address increases from 1 at the left to 768 at the right. Note that this convention is different from that used by the engineers (defined in Camera Operations Manual, IUE Technical Note 30).

read beam is pulsed on by the "G1 modulator" for 6 $\mu$ s, after allowing time for the deflection amplifiers to settle. The beam recharges the target, giving rise to an output video pulse corresponding to the positive charge on the target at that pixel. The analogue video signal, after pulse-shaping and amplification, is digitised into one of 256 discrete levels (referred to as digital data number or DN units) by an 8-bit analogue-to-digital converter. Two head-amplifier gain settings (HI and LO) are available; the HI setting has three times the gain of the LO setting and may be used to reduce the digitisation error for low-level signals.

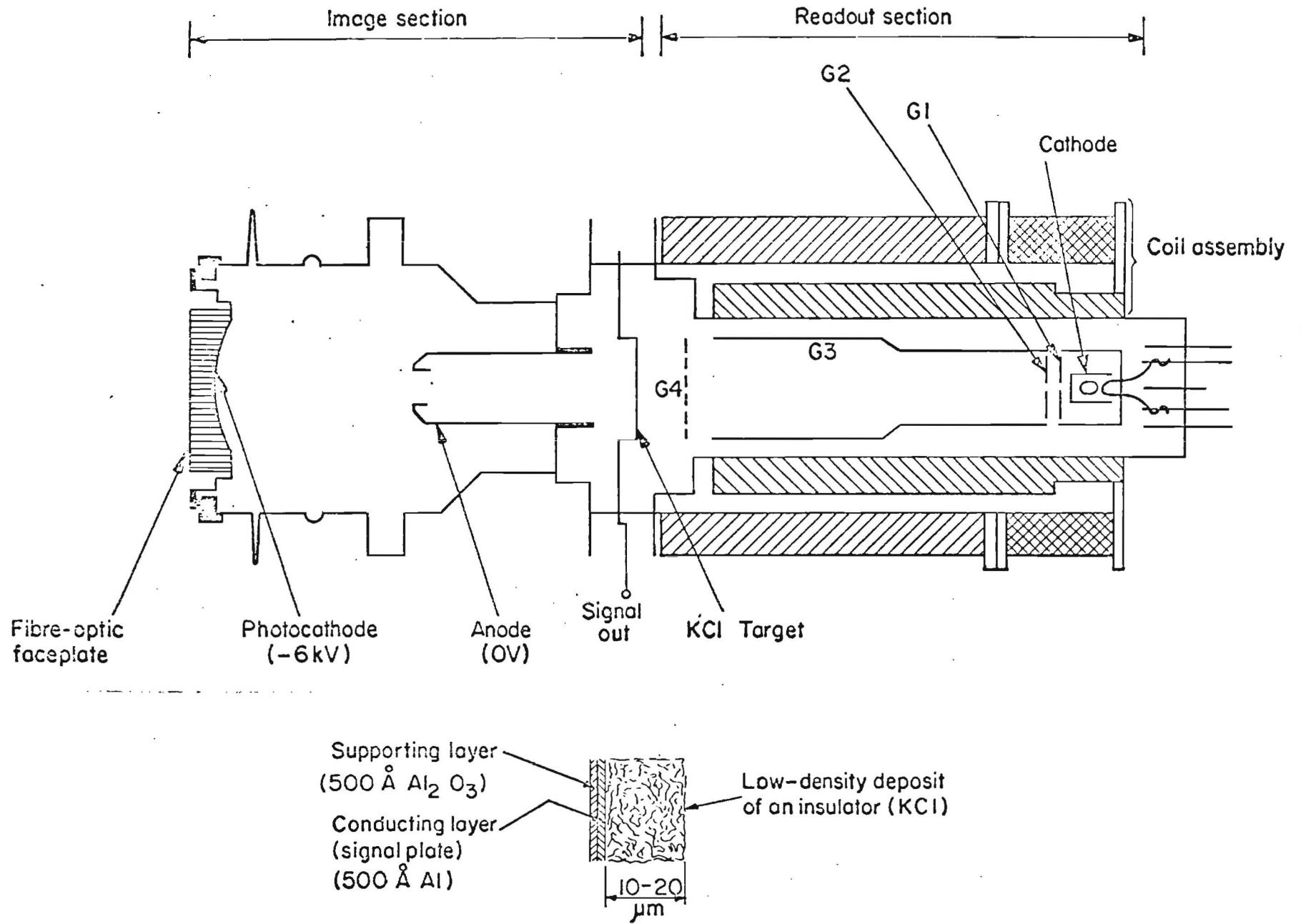


Fig. 2.2-1 The SEC television camera tube (upper); detail showing the SEC target (lower).

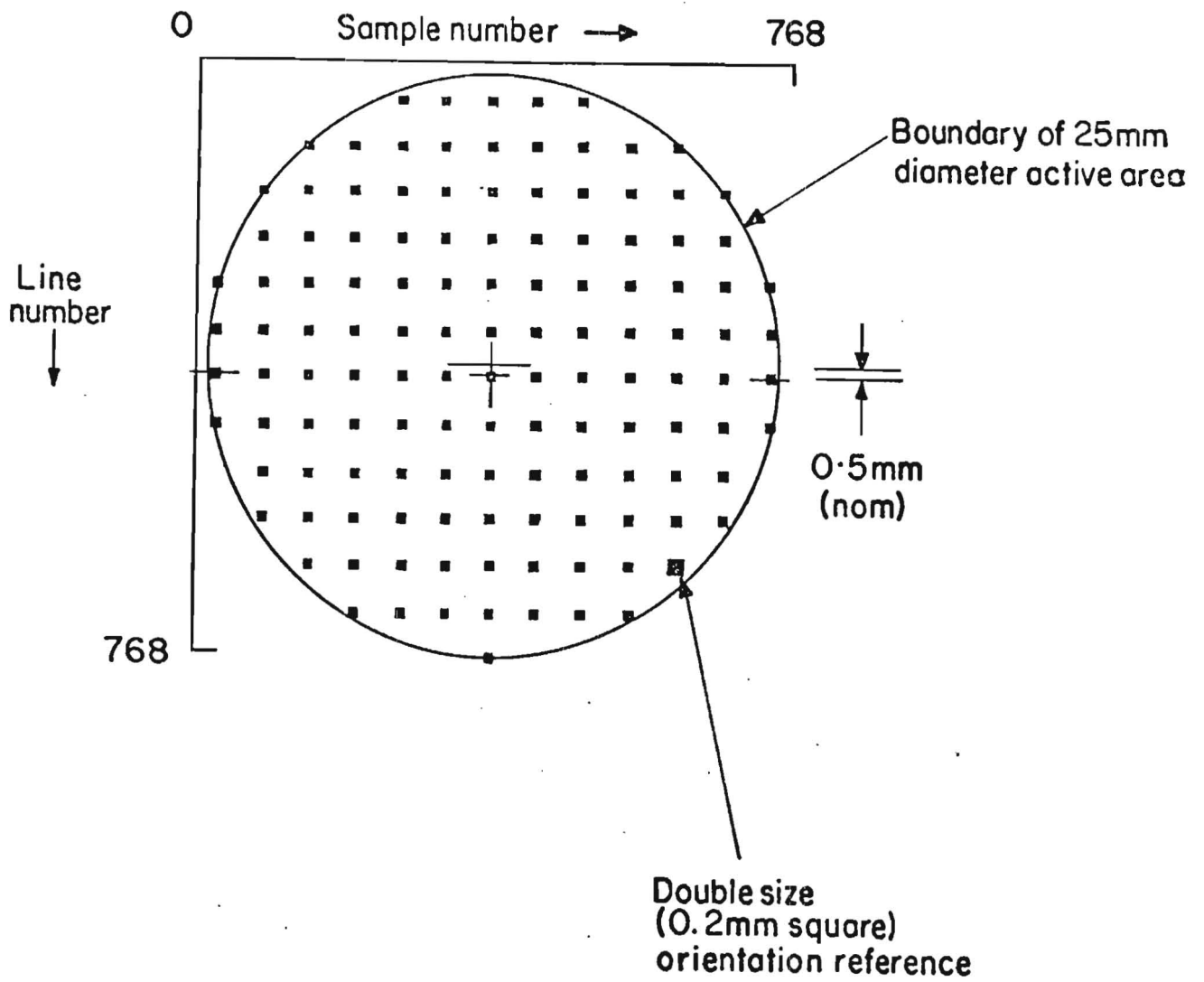


Fig. 2.2-2 Image display format, showing pixel addressing convention used by image processing software, and positions of fiducial marks.



### 2.3 Electronics

A camera sub-system is shown in block-diagram form in Fig. 2.3-1. Low voltage power supplies from the spacecraft are routed through the Camera Supply Interface Module (CSIM). The Camera Electronics Module (CEM) contains most of the electrode supplies for the SEC tube together with focus, deflection and alignment drives for the coil assembly. High voltages for the UVC and SEC tube image section are generated locally in the CHM. Other important constituents of the system electronics are the video signal chain and comprehensive status monitoring; the outputs from both of these functions are routed to the spacecraft telemetry system. The various camera operational modes and readout scan parameters are controlled by information from the Scan Control Logic (SCL) which is part of the Experiment Electronics Assembly (EEA).

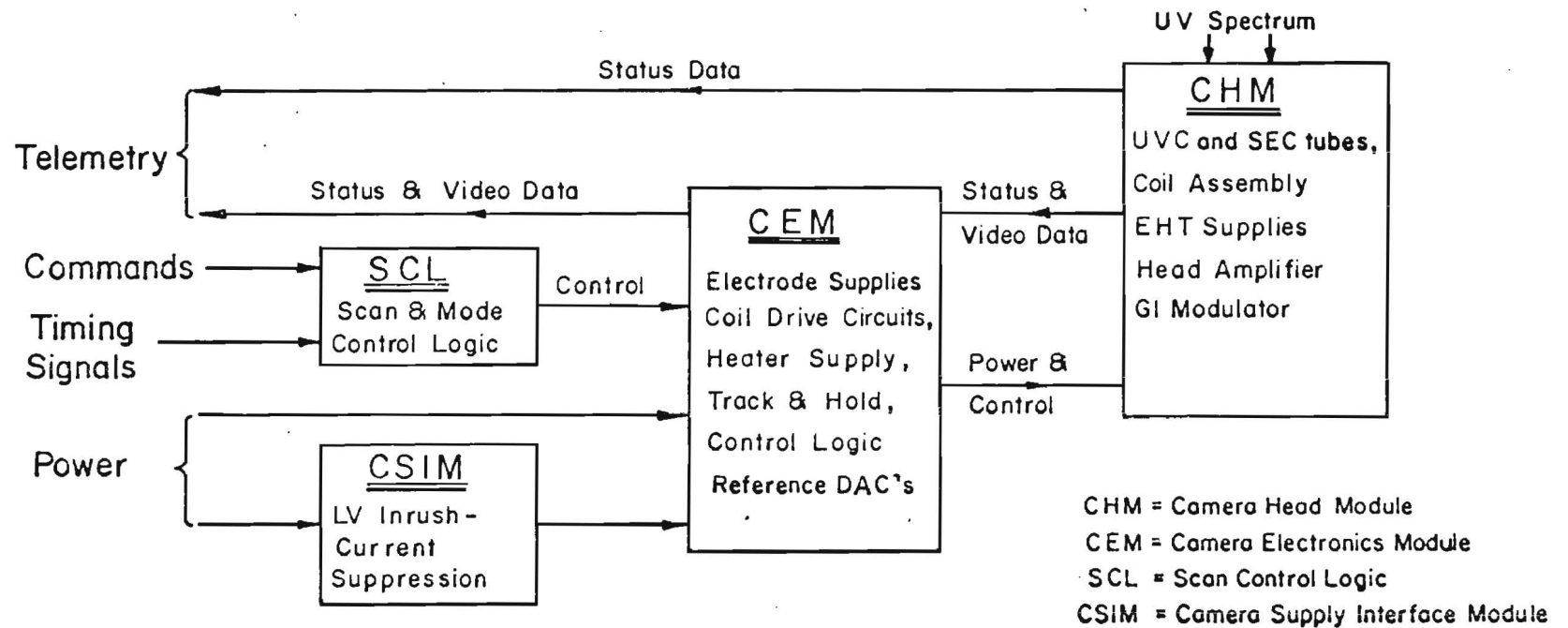


Fig. 2.3-1 Block diagram of IUE camera sub-system.

## 2.4 Camera Operating Sequences

Camera operating sequences are controlled by mode commands issued by the ground-station computer in response to keyboard procedure calls. Each operational mode may have one or more parameters which may be selected by the guest astronomer (§4). Any active mode is entered from and concluded by entry to the STANDBY mode. The normal image sequence (active modes only) is:

PREPARE  
EXPOSE  
READ

The modes are described below.

Note (i) It is generally only possible to operate with a single camera in any active mode at any one time.

(ii) There are certain operational situations which are either hazardous to the cameras or undesirable in that they may result in bad data and waste valuable observing time. The astronomer must be guided by the advice of ground station staff; the latter are the only persons authorised to enter procedure calls. Hazardous modes are fully documented in the Camera Operations Manual (IUE Technical Note 30).

### 2.4.1 STANDBY mode

The STANDBY mode is an indefinitely safe, power-conserving mode, into which a camera is configured immediately on switch-on and at all times when it is not in one of the active modes.

### 2.4.2 EXPOSE mode

An image may be integrated on the SEC target in this mode where UVC and SEC image section high voltages are on (the readout section of the SEC tube is off).

Exposure time, SEC image section gain (MAXG, MEDG or MING), spectrograph mode (wavelength range, entrance aperture, dispersion) and light source (stellar spectrum or on-board source such as wavelength calibration lamp or UV floodlamp) may be selected by the astronomer according to the needs of the observation.

Exposure times controlled by the on-board computer are reproducible to better than 0.1s; however, the finite rise and fall times of the high voltage supplies mean that absolute exposure times have an uncertainty of  $\sim 0.5s$ . Exposures of less than a few seconds' duration are not therefore recommended, except for "quick-look" purposes.

A possible operational hazard in this mode is over-exposure (§3.6).

#### 2.4.3 READ mode

In this mode, the stored charge image is read out from the SEC target as described above in §2.1. The readout section of the SEC tube is active, whilst the image section and the UVC are off. The astronomer may select HI or LO head-amplifier gain. In certain exceptional circumstances, other variations may be permitted. These are:

Scan format other than 768 x 768 pixels.

Pixel rate other than standard spacecraft telemetry rate.

Pixel size other than standard.

The telemetered video data are recorded on disc and then on magnetic tape at the ground station. The image is available for quick-look analysis (§6) within five minutes of completion of the READ operation.

#### 2.4.4 PREPARE SEQUENCE

A PREPARE operation is carried out before each EXPOSE in order to erase all trace of previous images, and to provide a reproducible low-noise pedestal or baseline on which the new image will be superimposed. Several PREPARE sequences are available; essentially, they all consist of pre-programmed sequences of exposures to the tungsten floodlamps followed by READ scans. The options are:

- (i) Normal PREPARE ("SPREP"), suitable for the majority of observations (Operation time  $\sim 10m$ ).
- (ii) Fast PREPARE ("FPREP"), for quick-look images and exposure time trials, where image quality is of secondary importance. (Operation time  $\sim 3m$ ).
- (iii) Low-noise PREPARE ("LNPREP"), for faint objects where highest signal-to-noise ratio is the most important consideration. (Operation time  $\sim 15m$ ).
- (iv) High-level PREPARE ("XPREP"), designed to be used following severely over-exposed images, and to precede SPREP or LNPREP where these alone would not provide sufficient erasure.

## 2.5 References

- 2-1. C I Coleman and A Boksenberg, *Contemp. Phys.* 17, 201-236 (1976).
- 2-2. A H Boerio, R R Beyer and G W Goetze, *Adv. Electron. Electron Phys.* 22A, 229 (1966).

### 3. CAMERA PERFORMANCE

#### 3.1 Sensitivity

The overall sensitivity of the IUE cameras is defined by the product of the photocathode quantum efficiency (QE) of the ultraviolet-to-visible converter (UVC) and the photoelectron sensitivity (S) of the rest of the system. Note that QE is wavelength-dependent whilst S is a wavelength-independent quantity.

##### 3.1.1 Quantum efficiency

The primary detection process in the IUE cameras involves the conversion of incident ultraviolet photons to photoelectrons by the UVC's caesium telluride photocathode. The QE (strictly speaking, the responsive quantum efficiency) of a photocathode is defined as the ratio of the number of photoelectrons produced to the number of incident photons.

QE is a function of the wavelength of the incident light; a typical spectral response for the IUE cameras is illustrated in Fig. 3.1-1. Peak QE is in the region of 0.2 over a large part of the useful spectral range. A notable feature of the spectral response curve is the dip centered on 150 nm; this is caused by pair-production energy loss processes in the photocathode (Ref. 3-1). At wavelengths shorter than 115nm, QE is limited by the falling transmission of the magnesium fluoride camera faceplate. Good rejection of long-wavelength scattered light beyond about 320 nm is provided by the steeply descending QE characteristic in this region; there is, however, a tail of residual sensitivity ( $QE < 10^{-3}$ ) extending out to fairly long wavelengths in the visible (in fact, the 400 → 500 nm response is important, because the tungsten filament floodlamps in the spectrograph emit virtually no ultraviolet radiation).

Because of the high electric field in the UVC ( $3.85 \times 10^6 \text{ V m}^{-1}$ ), the QE is considerably greater than in low-field devices using the same type of photocathode. This enhancement effect is particularly apparent in the threshold region around 300 → 330 nm, and on the short-wavelength side of the QE dip between 120 and 140 nm (Ref. 3-2).

Variations of QE across the image area do exist in the IUE cameras, but are fairly small, typically less than ±5%. Such variations, which are generally slow functions of position, are corrected using the image calibration files in software.

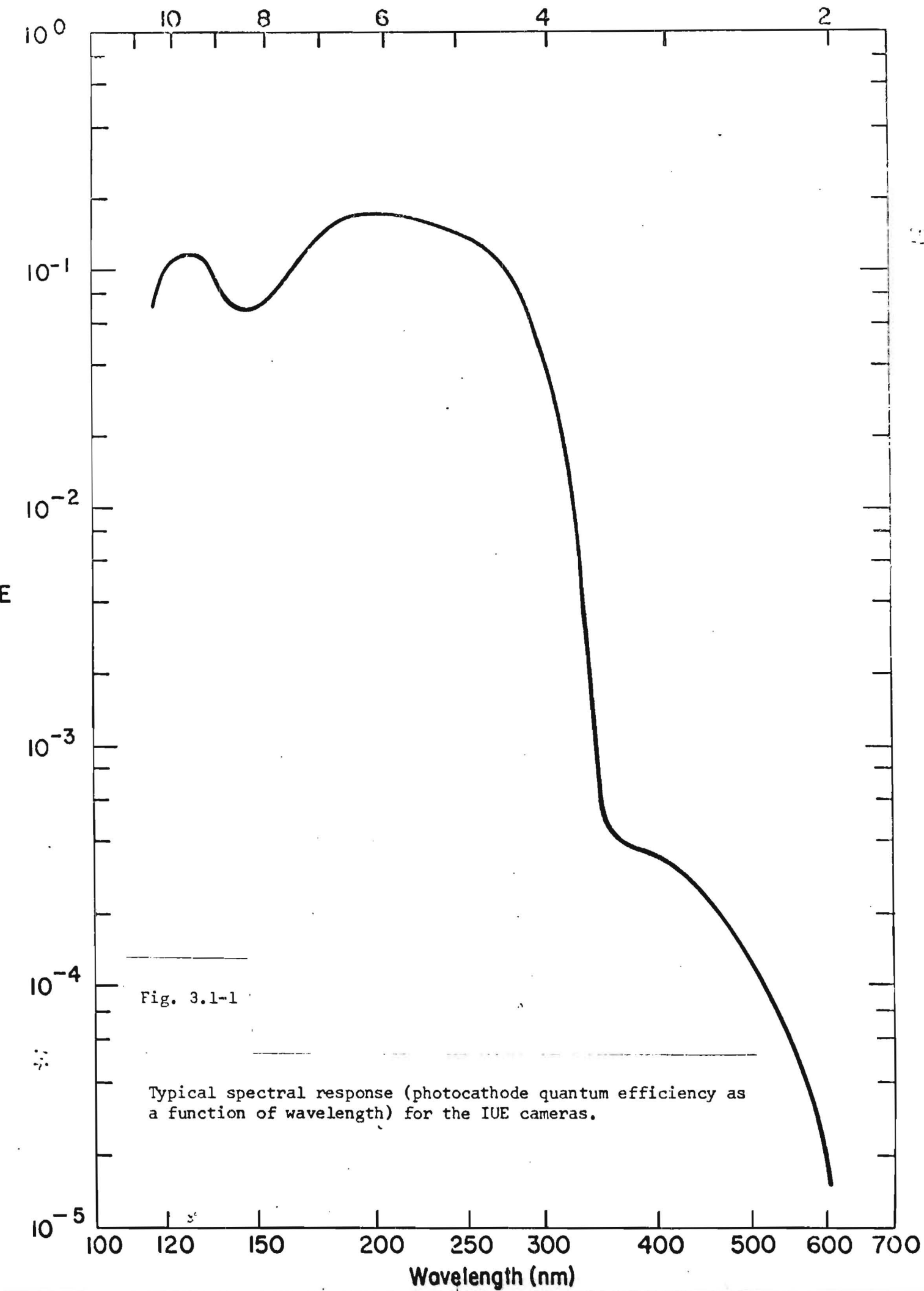


Fig. 3.1-1

Typical spectral response (photocathode quantum efficiency as a function of wavelength) for the IUE cameras.

### 3.1.2 Photoelectron sensitivity and intensity transfer function (ITF)

The response of a camera to photoelectrons produced at the photocathode of the UVC is non-linear at high signal levels. This is due to saturation effects in the storage of charge in the SEC target (the UVC is a linear device). Slight non-linearity at low signal levels is also occasionally apparent (this may arise from incorrect settings of operating parameters or from small drifts in the pedestal level on which images are superimposed). The relation between the output from the video chain and the number of input photoelectrons is known as the intensity transfer function (ITF) (Fig. 3.1-2). This varies from pixel to pixel ("fixed-pattern noise"), and its correction is an important element of data reduction. The ITF may be formally expressed by the following equation:

$$DN = A \cdot I(n, G_c, G_s) + DN_0 \quad (1)$$

where DN = digitised output signal from the video chain.

$DN_0$  = "null" level, i.e. the output signal for zero exposure (note that the null level varies somewhat with position in the image).

$n$  = number of incident UVC photoelectrons per pixel (pixel area =  $1.3 \times 10^{-3} \text{ mm}^2$ ).

$A$  = video chain sensitivity with head-amplifier in LO gain (= 0.0014 DN per electron read out from the target). Note that with head-amplifier in HI gain, the sensitivity is  $3A$ .

$G_c$  = coupled electron gain of UVC and SEC, i.e. number of photoelectrons produced at SEC photocathode for each UVC photoelectron. (This is not strongly dependent on position in the image, but is a function of UVC voltage; the latter is normally fixed at 5 kV and  $G_c$  is then typically equal to 6).

$G_s$  = low-signal gain of SEC target, i.e. the number of stored charges produced per incident photoelectron (on the linear part of the ITF curve). This is a function of the SEC image section voltage during EXPOSE and varies typically from 5 at MING to 15 at MEDG and 50 at MAXG. It is also a function of image position and of the operating parameters used for PREPARE and READ.

$I(n, G_c, G_s)$  is a non-linear function of  $(n, G_c, G_s)$ . This function is strongly dependent on image position.



At low to medium signal levels, the ITF is linear and:

$$I(n, G_c, G_s) \approx n \cdot G_c \cdot G_s \quad (2)$$

Equation (1) then reduces to:

$$DN - DN_0 = n \cdot S \quad (3)$$

where  $S = A \cdot G_c \cdot G_s$ .

S (expressed in DN per photoelectron per pixel) is termed the photoelectron sensitivity of the camera; its magnitude is given by the gradient of the broken lines in Fig. 3.1-2. The sensitivity is a fairly strong function of position in the image, both on a pixel-to-pixel scale (due to structure in the SEC target) and on a large scale (believed to be due to asymmetries in the construction of the SEC tube or coil assembly). A typical sensitivity map across the face of a camera is shown as a contour plot in Fig. 3.1-3.

Sensitivities (DN per photoelectron per pixel) are tabulated below for the four cameras. The figures apply for EXPOSE with SEC MAXG and READ with LO gain. The sensitivities are lower by factors of  $\sim 3$  and  $\sim 10$  respectively at MEDG and MING, and are three times higher with READ in HI gain.

Spectrograph position	Camera serial no.	Sensitivity (S)
Long- $\lambda$ prime	06	0.25
Long- $\lambda$ redundant	07	0.35
Short- $\lambda$ prime	08	0.35
Short- $\lambda$ redundant	09	0.25
(Flight spare)	05	0.45

These photoelectron sensitivities should be multiplied by the QE at the wavelength of interest in order to obtain the overall camera sensitivity in DN per photon per pixel. Note however that it will generally be more useful to consider the QE as part of the wavelength-dependent sensitivity of the whole system (telescope/spectrograph/photocathode) and to treat the wavelength-independent but intensity-dependent photoelectron sensitivity separately (see §4).

*red sensitivities calculated from "IUE Camera Data Summary" prepared by C.I. Coleman, 11 Aug 1977.*

TN 31/1

AVH

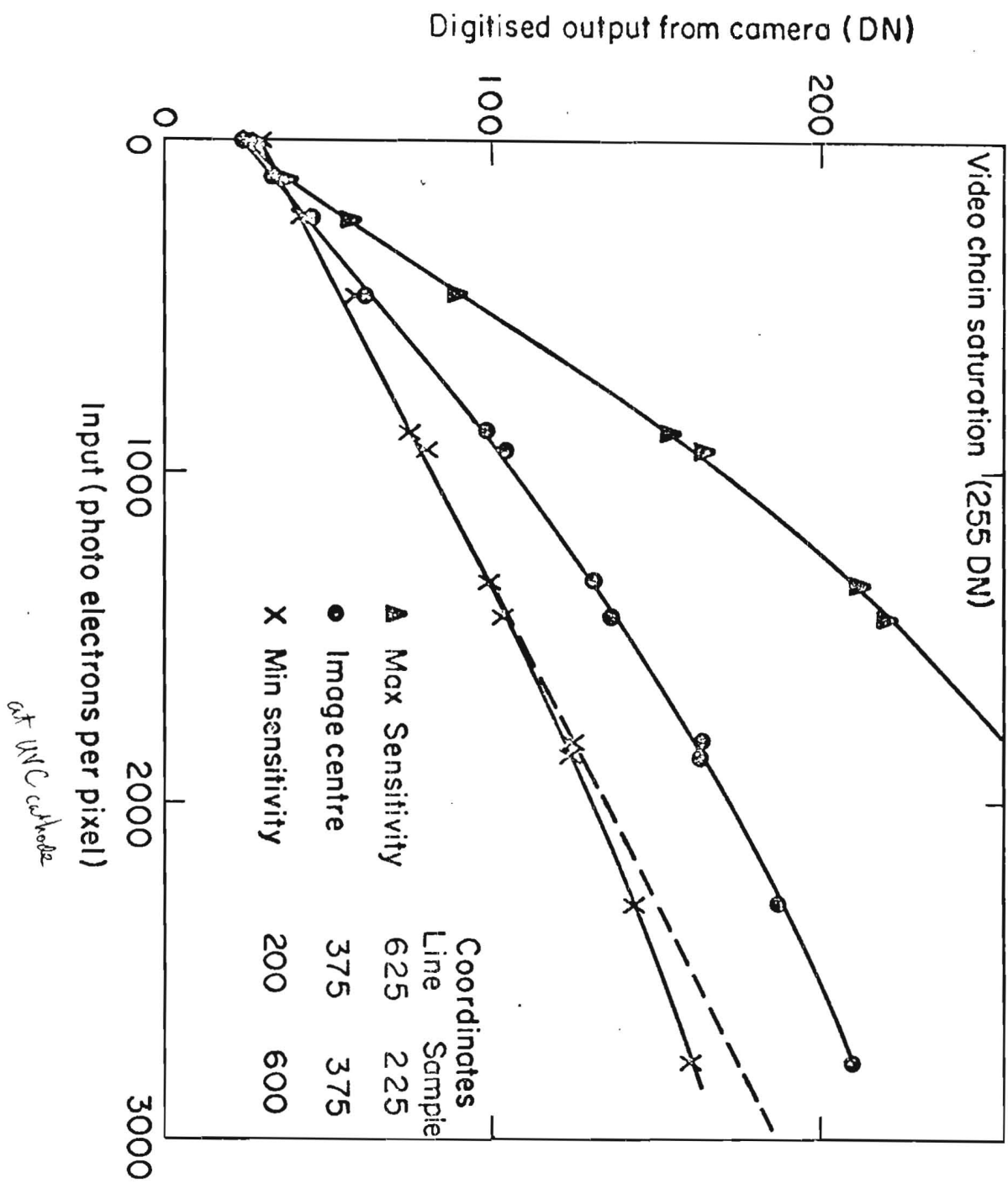


Fig. 3.1-2 Intensity transfer function (ITF) for the image centre and the positions of maximum and minimum sensitivity, for the short-wavelength prime camera (SEC MEDG, READ in LO gain).

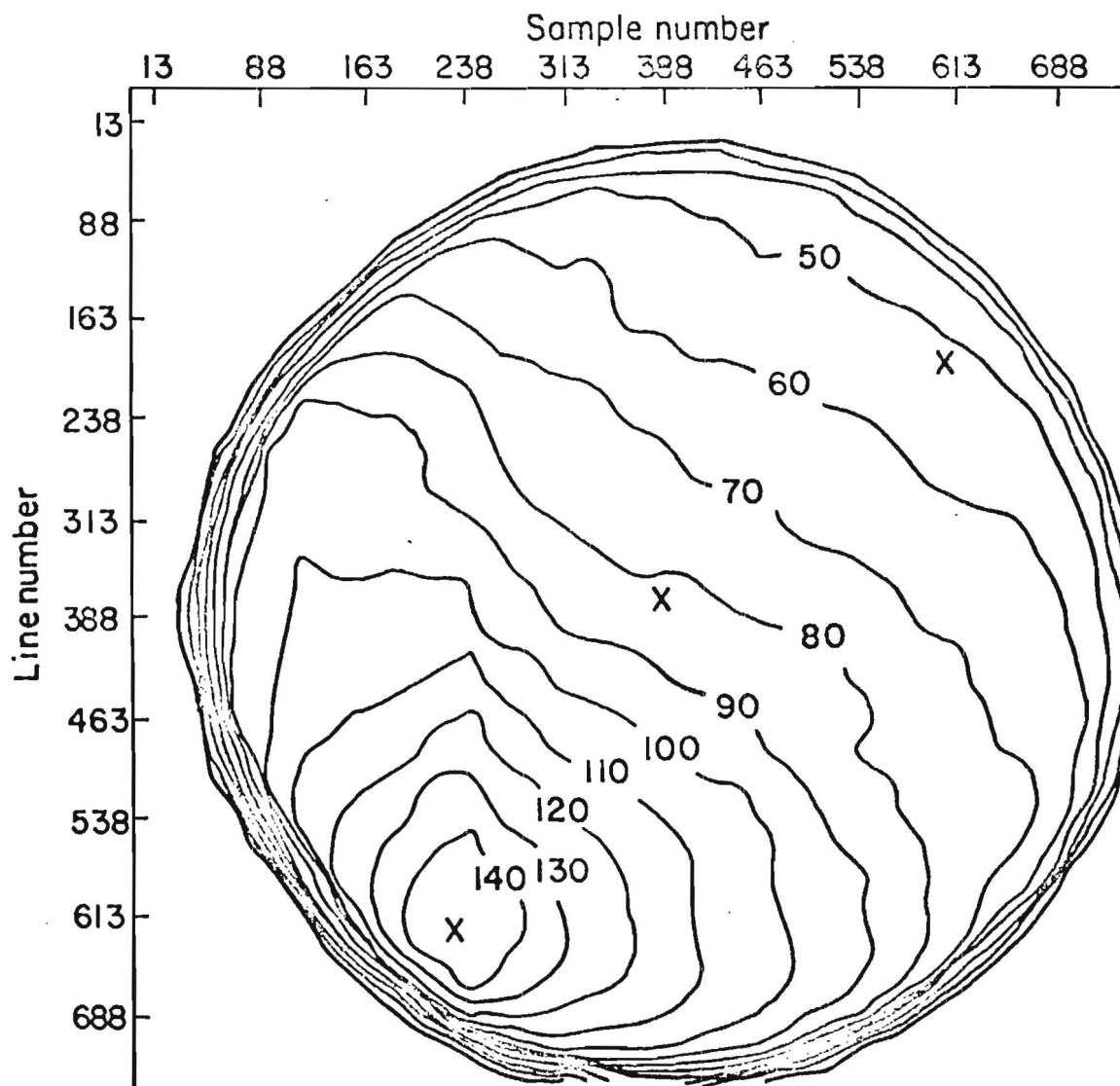


Fig. 3.1-3 Map of sensitivity variations across the image (short-wavelength prime camera, SEC MF DG). Contours are labelled in units of DN per 100 photoelectrons. X marks the locations of the points for which ITFs are plotted in Fig. 3.1-2.

### 3.2 Signal-to-Noise Ratio and Dynamic Range

Sensitivity alone is insufficient to define the accuracy with which a spectral feature may be measured; one must also consider the noise in the image (Ref. 3-3). The fundamental limit of accuracy is set by the quantum statistics of the photons incident on the detector. Any real detector falls short of this limit. In the IUE cameras, noise is dependent upon such parameters as SEC target gain, signal level, type of PREPARE sequence, and wavelength; further, it varies somewhat from one camera to another.

Unless otherwise stated, signal-to-noise ratio (S/N) will be defined as signal amplitude to RMS noise ratio after photometric correction ("ITF correction"). As ITF correction (§5.5) removes fixed-pattern noise, S/N is a measure of the random noise in an image and in the ITF table. S/N is shown as a function of SEC target gain (MAXG, MEDG or MING) and head-amplifier gain in READ (HI or LO) for the centre of the image in Fig. 3.2-1. The curves have been terminated once the signal in the lower left quadrant of the image reaches the telemetry limit (255 DN). The SEC MING setting is useful for objects which are too bright for MEDG or MAXG (§4). Use of HI gain on the head amplifier during READ decreases digitisation errors by a factor of 3. For weak signals, this can increase S/N by 10% to 15% for some cameras. However, dynamic range is thereby reduced and this may offset the advantage of slightly improved S/N.

In Fig. 3.2-2 the variation of S/N over the image area for MEDG is shown. A "flat-field" input (a uniform monochromatic beam of light) at 253.7 nm was used, and the exposure level was about 60% of full scale.

In Figs 3.2-3 and 3.2-4, S/N for the four flight cameras and for the prime spare (05) is compared at SEC MAXG and MEDG. The four flight cameras have similar performance.

S/N varies over the image area but the central parts of the pictures, used for Figs 3.2-3 and 3.2-4, give representative values for the mean S/N in an image.

The dynamic range (the range of input signals for which the S/N is greater than or equal to a given value) is listed for the central part of each camera in Table 5.2-1 for the values  $S/N \geq 10$  and  $S/N \geq 25$  (the figures apply for a spectral element of  $3 \times 3$  pixels).

The random noise in a spectral image after ITF correction ( $\sigma_R$ ) is a combination of the random noise in the ITF table ( $\sigma_{R,T}$ ) and the random noise in the spectrum ( $\sigma_{R,S}$ ):

$$\sigma_R^2 = \sigma_{R,T}^2 + \sigma_{R,S}^2 \quad (1)$$

Averaging  $n$  images decreases the random noise in the averaged image by  $n^{\frac{1}{2}}$ . The ITF calibration files are, at present, built up from single images; averaging more than 2 or 3 spectra is therefore a waste of time as  $\sigma_R$  can never be lower than  $\sigma_{R,T}$  and, for the same exposure level,  $\sigma_{R,S} \lesssim \sigma_{R,T}$ .

Averaging  $P$  pixels in a single image does not decrease noise by  $P^{\frac{1}{2}}$  because (i) the image of each detected photon is spread out over several pixels (§3.3) and photon noise in adjacent pixels is correlated (averaging  $3 \times 3$  pixels decreases noise at low and medium exposure levels by typically a factor of 2.0 to 2.5), and (ii) due to the destructive nature of the readout process from the SEC target, read beam pointing errors give rise to noise which is anticorrelated between adjacent pixels; anticorrelated errors cancel when pixels are averaged and noise decreases as  $P^{\frac{3}{2}}$  after averaging  $P$  pixels. For high exposure levels, averaging  $3 \times 3$  pixels improves S/N by a factor of 3 to 5.

As a consequence of the software correction for geometrical distortion (§§3.4 and 5.4), signal is redistributed and noise is smeared out over adjacent pixels. S/N increases after averaging over an area of  $N \times M$  pixels by:

$$[NM]^{\frac{1}{2}} * \left[ \frac{3N}{(3N-1)} * \frac{3M}{(3M-1)} \right]^{\frac{1}{2}}. \quad (2)$$

Here, the first term describes the classical square-root behaviour of random noise, and the second term the geometrical smearing process. Formula (2) gives an increase in S/N per single pixel of 50% through geometrical effects alone, and per resolution element ( $3 \times 3$  pixels) by a factor of 3.38.

Formula (2) does not incorporate pixel-to-pixel correlation or anti-correlation of noise, and it therefore overestimates the S/N increase for  $N * M \lesssim 9$ .

Table 3.2-1

Dynamic Range for S/N greater than 10 and 25

Camera	Slot	SEC target gain setting	Dynamic range for S/N	
			≥ 10	≥ 25
05	-	MAXG	17:1	3.5:1
		MEDG	25:1	6.2:1
06	LWP	MAXG	6.8:1	2.4:1
		MEDG	13:1	4.0:1
07	LWR	MAXG	-	-
		MEDG	28:1	4.4:1
08	SWP	MAXG	-	-
		MEDG	21:1	5.9:1
09	SWR	MAXG	-	-
		MEDG	15:1	4.6:1

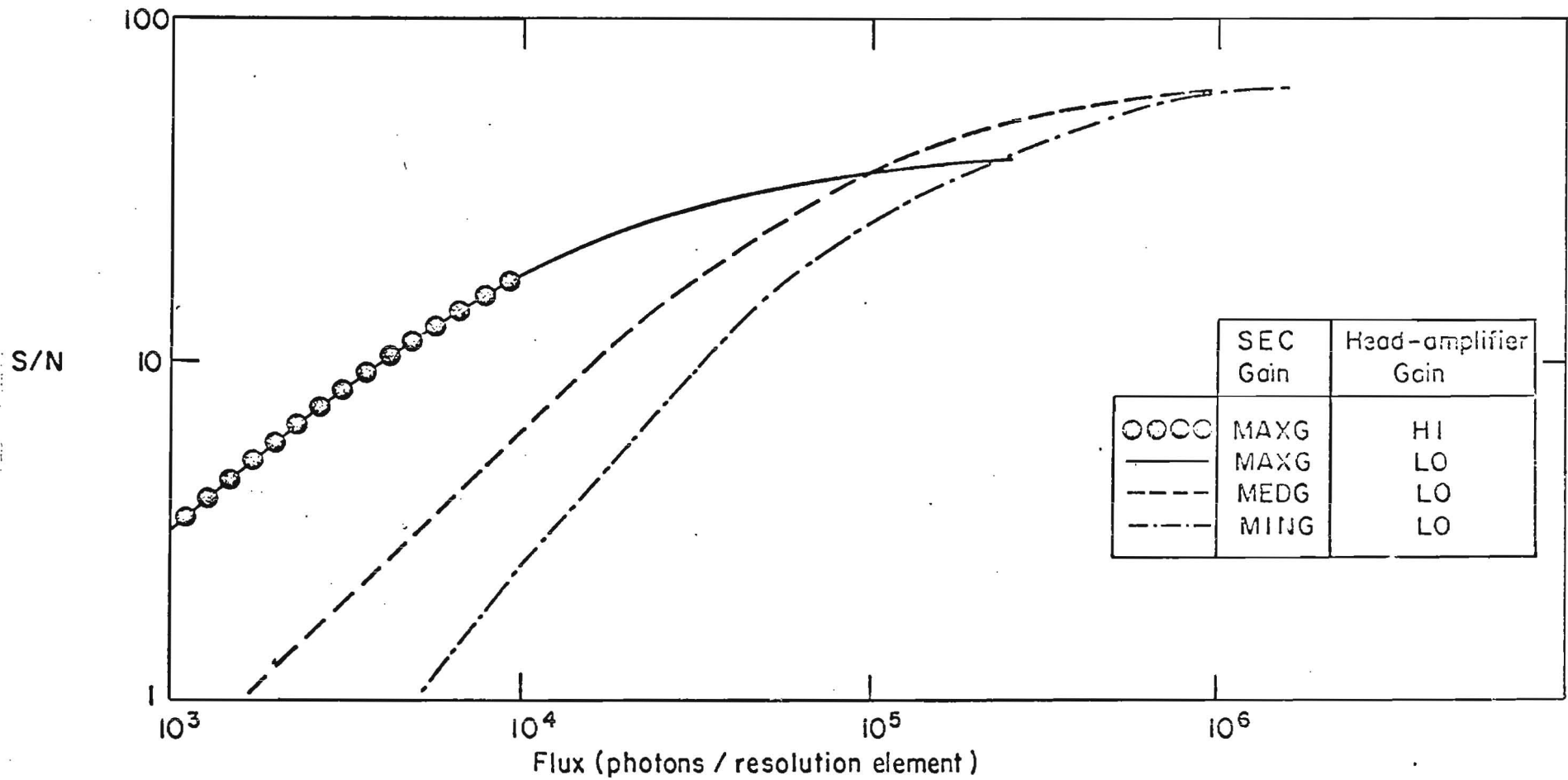


Fig. 3.2-1 Signal-to-noise ratio as a function of exposure level (254 nm photons per 3\*3 pixel resolution element). (Qualification model camera; Prepare sequence NPREP).

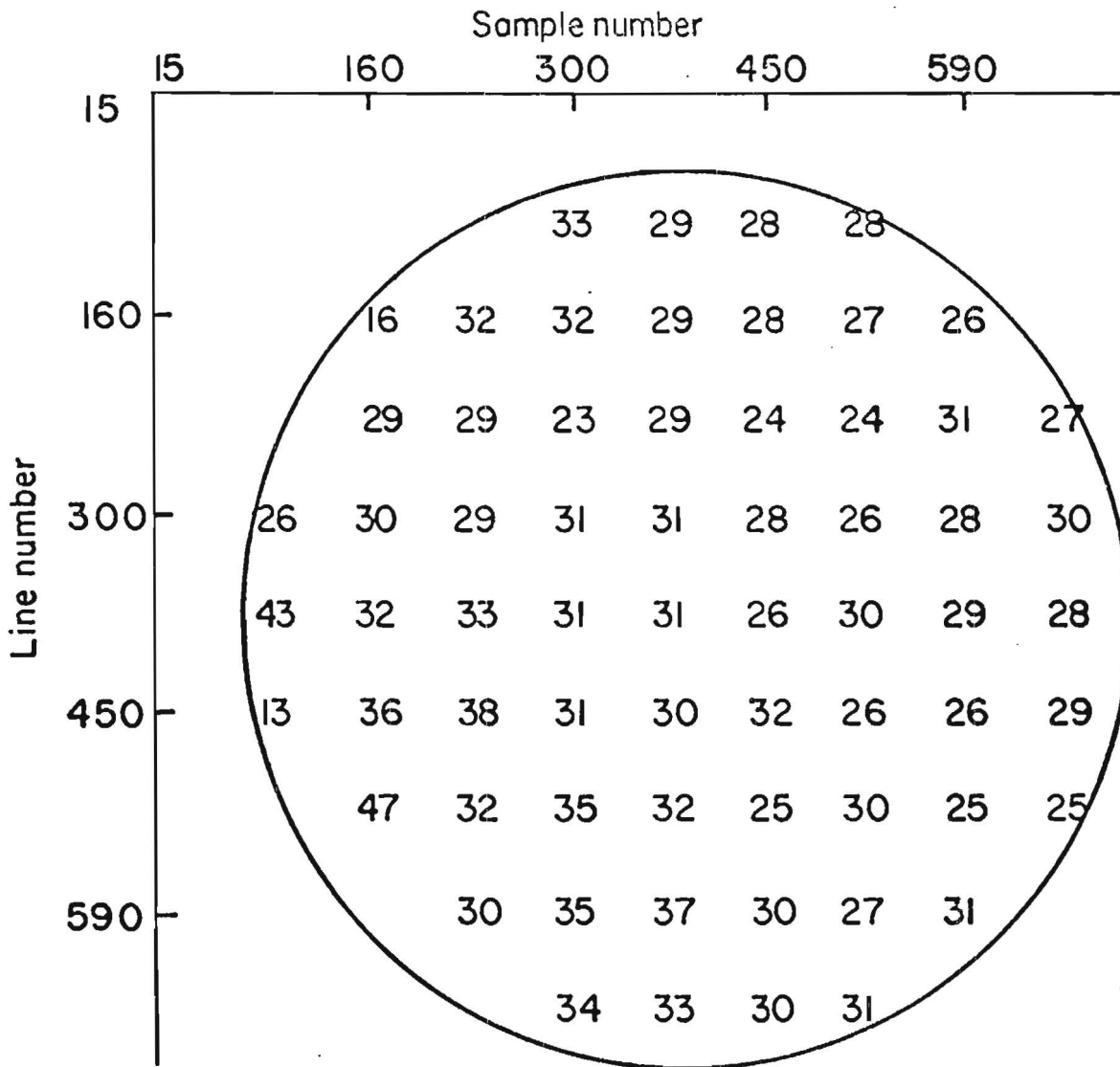
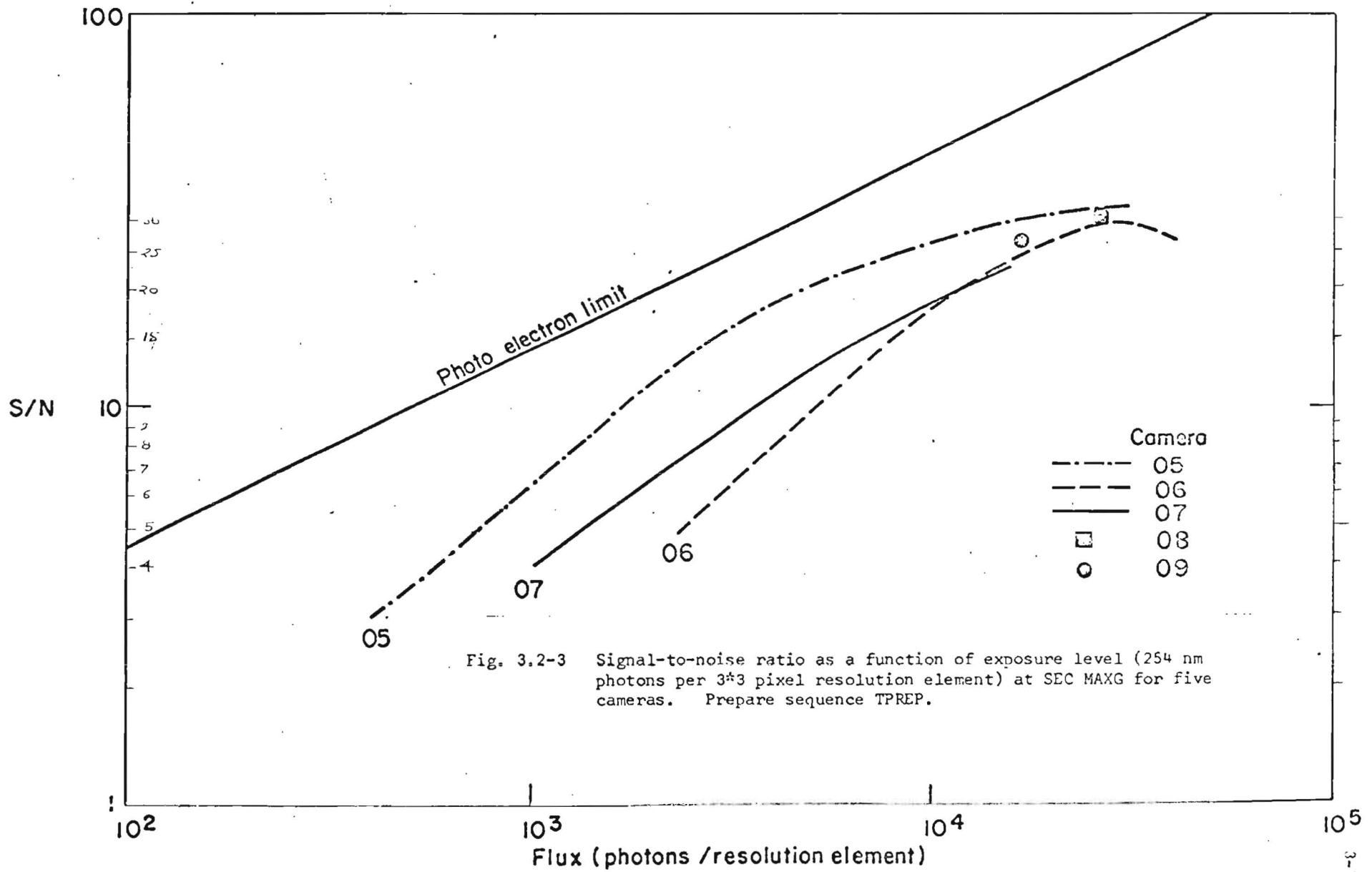
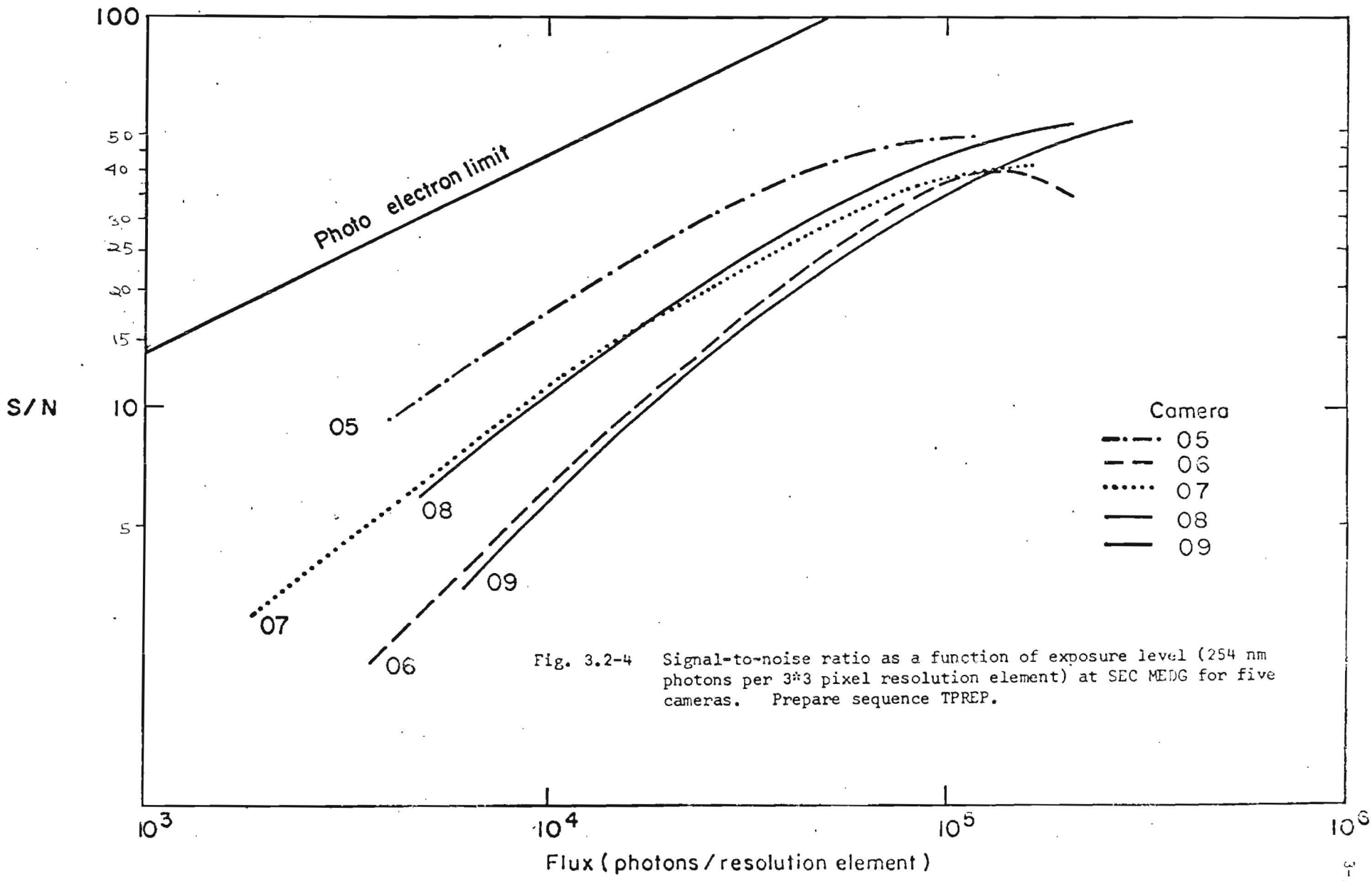


Fig. 3.2-2 Variation of signal-to-noise ratio per resolution element over the image area (Camera 04, Prepare sequence TPREP, ~60% flat-field exposure (254 nm) at SEC MEDG).







### 3.3 Resolution

The resolution of the IUE Scientific Instrument is determined by the combination of the camera resolution, discussed here, and the imaging quality of the optics (§00.00).

The camera point spread function (PSF), is determined by convolution of the PSF of the UVC with that of the SEC tube. The result is a camera PSF with a narrow, nearly gaussian core and a weak long range 'tail' due to halation. The full width at half maximum (FWHM) of the core and the amount of halation depend mainly upon wavelength, position in the image and SEC target gain; in addition, there are small variations from camera to camera. In Fig. 3.3-1, two MTFs are shown together with the central regions of the corresponding PSFs. (Modulation transfer function (MTF) is a measure of the resolution performance of the system as a function of spatial frequency; it is related by a Fourier transform to the line spread function and by a Hankel transform to the PSF). The image centre is representative of regions of good resolution; minimum resolution is reached in the bottom left area of the image. The very fast drop in the MTF at low spatial frequencies is due to halation; its magnitude is about 20% in the examples shown.

#### 3.3.1 The central core of the PSF

The central core of the camera PSF may be described by a gaussian having a FWHM of between 2 and 5 pixels, depending upon image position, wavelength, etc. The form of the wavelength dependence (Ref. 3-3) is illustrated in Fig. 3.3-2. There is a pronounced drop in resolution starting at  $\sim 240$  nm, reaching a minimum at 170 nm, and then increasing towards still shorter wavelengths. The initial drop is caused by the increasing energy of the photoelectrons released from the  $\text{Cs}_2\text{Te}$  photocathode by photons of increasing energy; at the shorter wavelengths ( $< 170$  nm), significant numbers of photoelectrons lose energy by pair production (Ref. 3-1; see also §3.1.1) and resolution improves again. The FWHM of the PSF can increase by up to 40% on going from 254 nm to 170 nm; at 122 nm, the resolution recovers and the FWHM is typically only 10% larger than at 254 nm.

### 3.3.3 Astronomical implications

The influence of the 'gaussian' core of the instrumental PSF on astronomical data is well known, and analysis of narrow spectral lines from IUE data will eventually result in a table of FWHM as a function of position and wavelength and, if necessary, SEC tube gain.

Halation in the images influences especially sharp narrow lines. Part of the line intensity is scattered all over the image and, as the faint line wings are invariably lost in the noise, the equivalent width will be systematically too low. For a narrow, sharp interstellar line at 121.5 nm, exposed at MEDG and in a region of the image having good resolution, the effect is small - perhaps 5% or less - but at 253.6 nm, using MAXG and in a region of lower resolution, the equivalent width can be perhaps 20 to 40% underestimated. Due to the rapid fall-off in halation intensity with distance, the under-estimation of equivalent width is much less for broader lines.

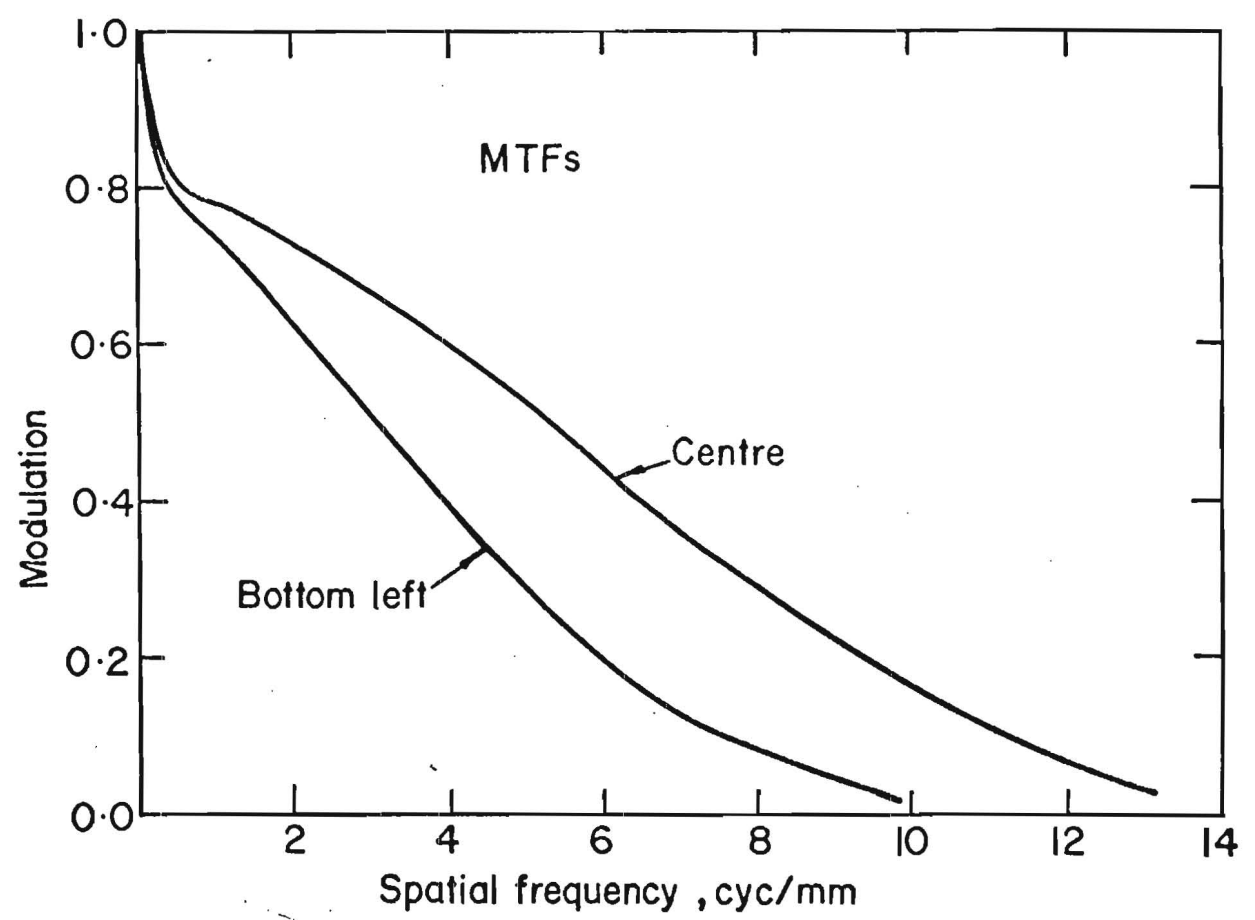
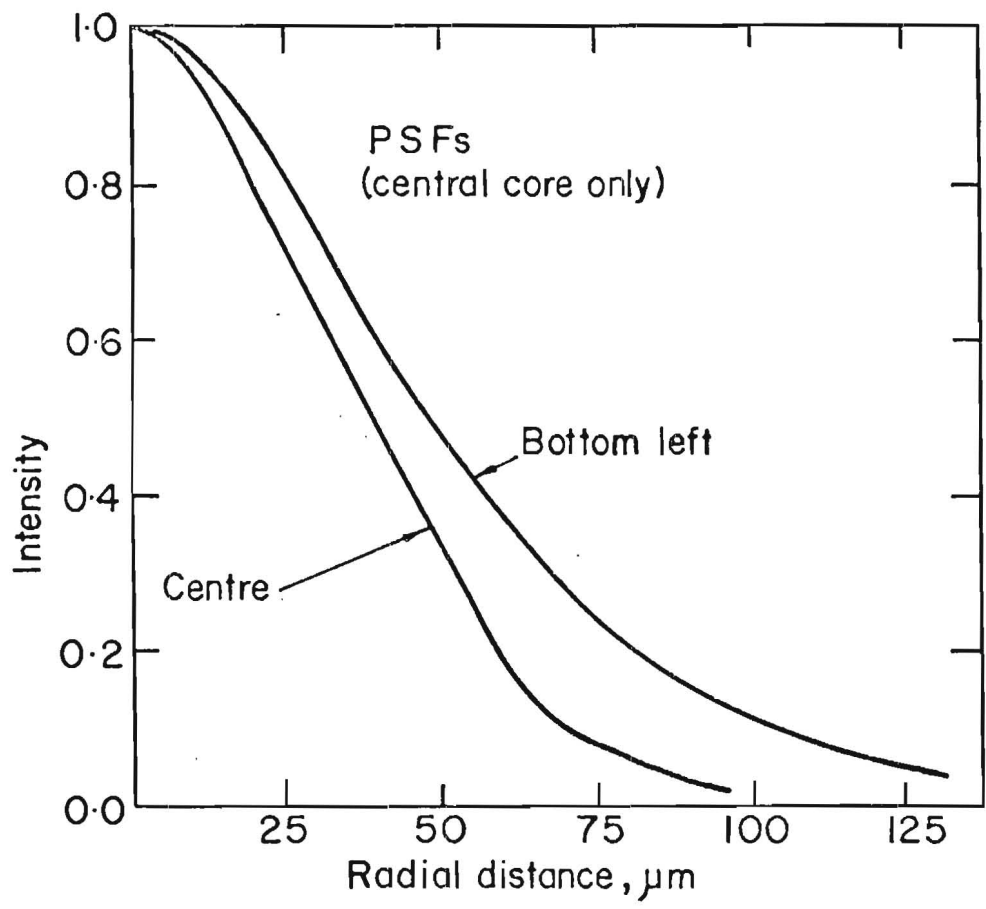


Fig. 3.3-1 Point spread functions (upper) and modulation transfer functions (lower) for centre of image and at half-radius. (TPREP, SEC MAXG,  $\lambda = 254 \text{ nm}$ ).

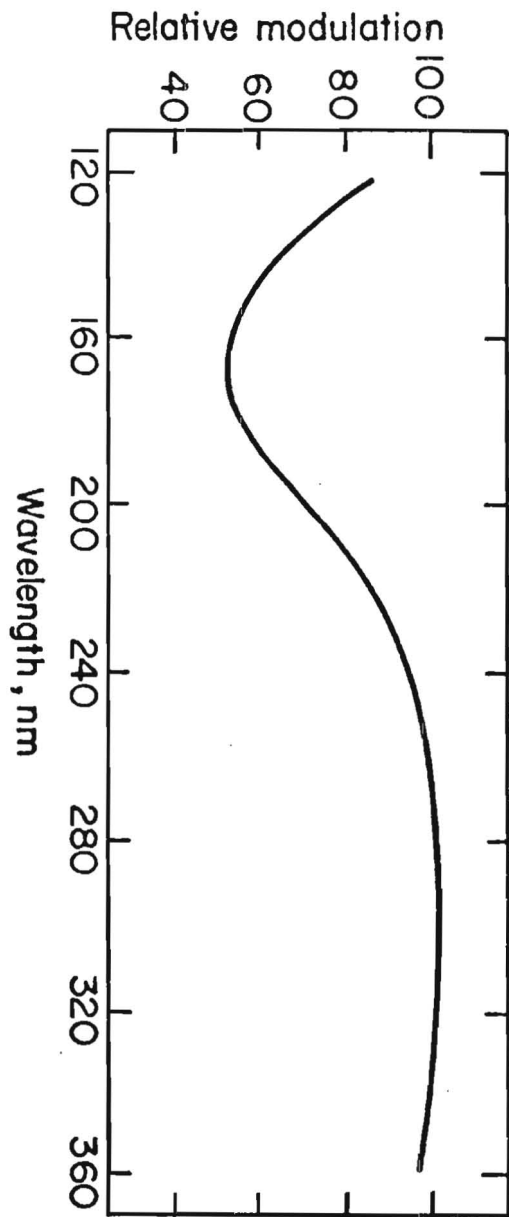


Fig. 3.3-2 Dependence of resolution on wavelength. The relative modulation at different wavelengths is approximately the same at all spatial frequencies.

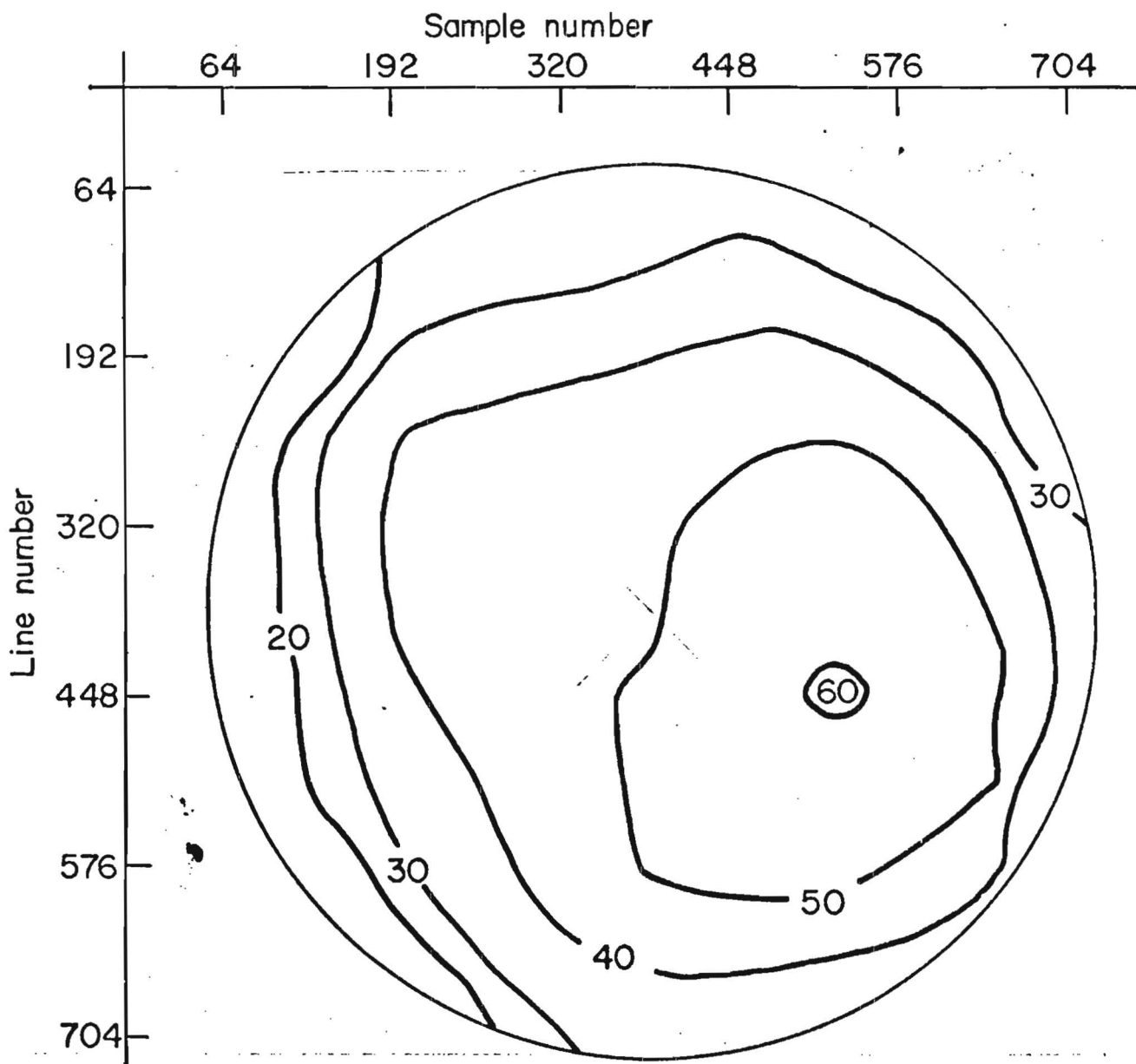


Fig. 3.3-3 Typical variation of resolution over the image area. (Contours of equal percentage modulation at 4,5 cyc/mm, TPREP, SEC MAXG,  $\lambda = 254$  nm).

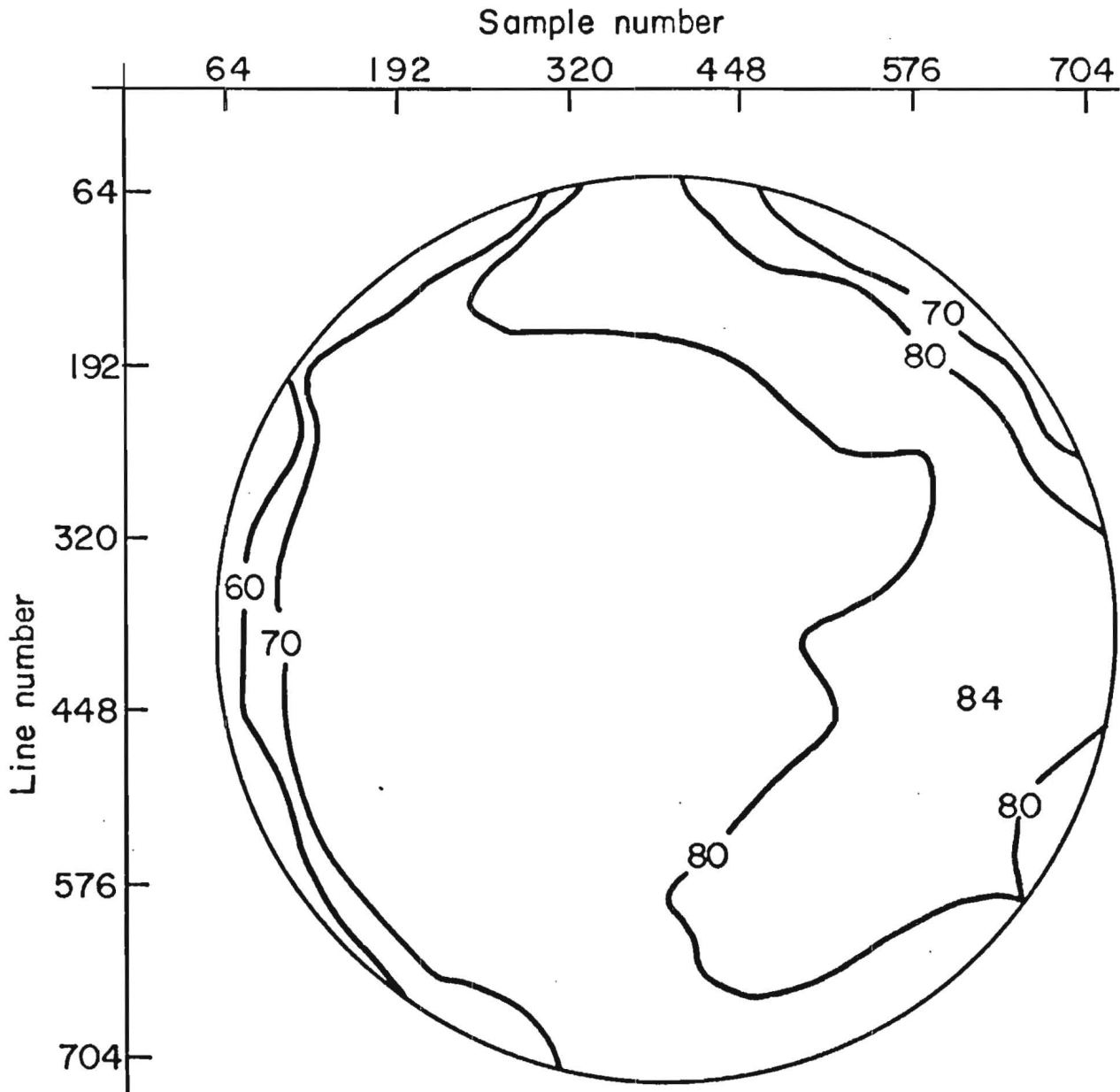


Fig. 3.3-4 Typical variation of halation over the image area at 254 nm.  
 (Contours of equal percentage modulation at 0.5 cyc/mm, TPREP,  
 SEC MAXG).



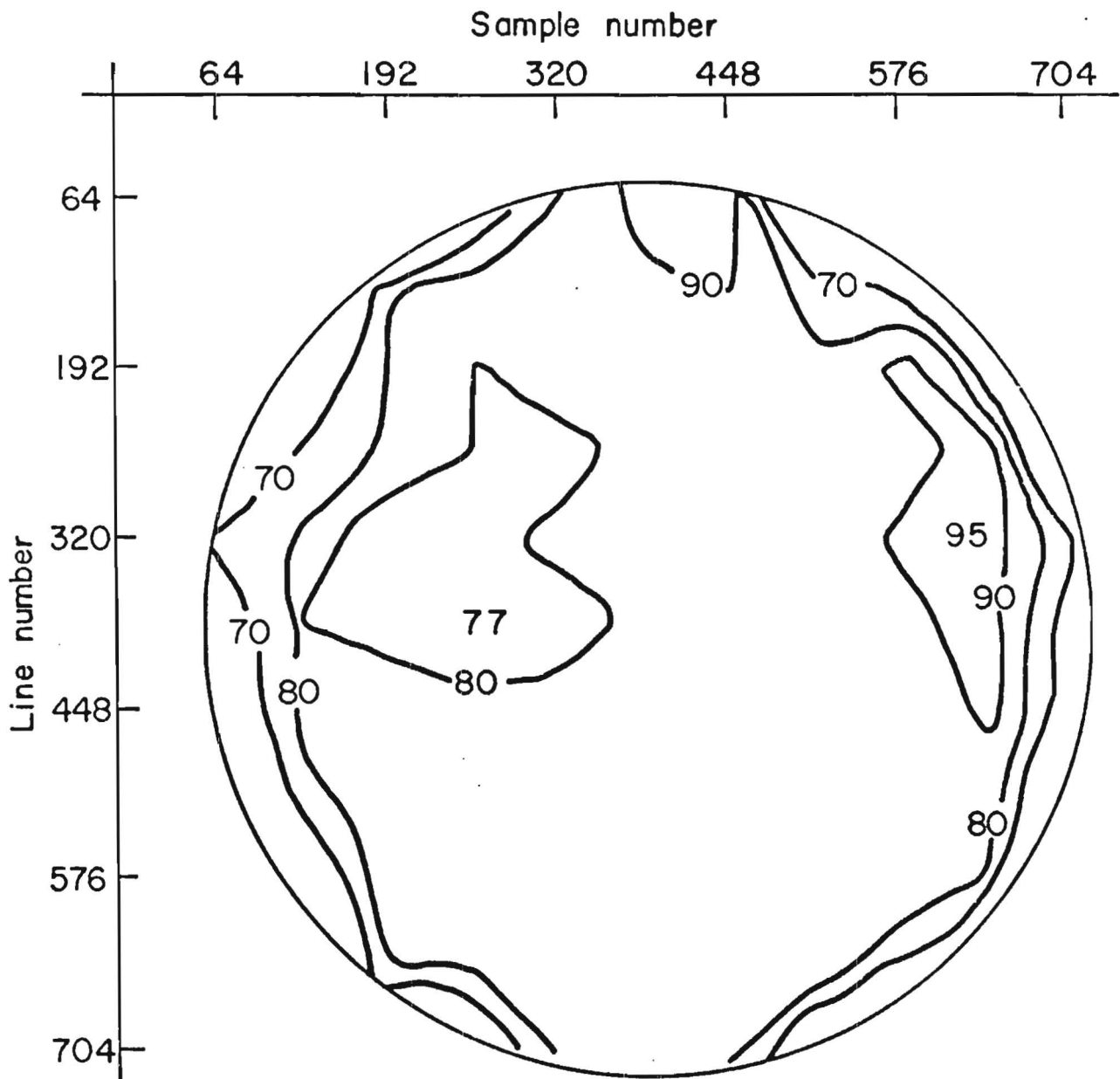


Fig. 3.3-5 Typical variation of halation over the image area at 122 nm (Contours of equal percentage modulation at 0.5 cyc/mm, TPREP, SEC MAXG).

3-13

The SEC image section electron optics give best resolution at the image centre; there is also an improvement in resolution (particularly at the image edges) with increasing EHT; the FWHM of the PSF decreases by a maximum of 15% between MING and MAXG. Further asymmetric position-dependent effects, producing reduced resolution in the lower left area of the image, arise in the readout section of the SEC tube. Variation of modulation at 4.5 cyc/mm over the image area (for illumination at 254 nm, exposed at MAXG) is shown in Fig. 3.3-3.

### 3.3.2 Halation

The strength of the tail of the PSF decreases with decreasing wavelength and with decreasing SEC tube gain. At 254 nm and MAXG, halation at the image centre amounts typically to 20% of the total energy, the UVC and the SEC tube contributing roughly 10% each.

Scattering of UV photons inside the UVC causes 7 to 8% halation at 254 nm and, at most, 1 or 2% at 122 nm. Electron backscattering from the anti-halation layer is responsible for a few percent halation; this latter process has a relatively short range, limited to 2.6 mm. Other scattering processes in the UVC, e.g. multiple reflections in the  $MgF_2$  faceplate, are negligible compared to the two mechanisms discussed above.

Representative values for halation in the SEC tube (at the image centre) are 8 to 10% at MAXG, 4 to 7% at MEDG and a very few per cent at MING. Halation in the SEC tube is position-dependent, and in regions of good or bad resolution, the halation can be a factor of 2 to 3 better or worse than the centre values listed above.

Figs. 3.3-4 and 3.3-5 show modulation at 0.5 cyc/mm for 254 nm and 122 nm respectively.

With the exception of the component due to electron backscattering in the UVC, halation intensity decreases approximately as the square of the distance from the source.

Typical halation performance is illustrated in Figs 3.3-4 and 3.3-5 which show modulation at 0.5 cyc/mm for 254 nm and 122 nm respectively.

### 3.4 Geometrical Distortion

Uncorrected images from the IUE cameras exhibit a small amount of image distortion (typically 2% of radial distance); this consists of a pincushion component from the SEC image section electron optics and an S-distortion component from the magnetically-focused readout section. There is also a slight change in image scale across boundaries distant 115 and 250 pixels from the centre line of the image in both sample and line scan directions (this is due to the method used for keeping the scanning electron beam in focus across the whole image area during READ); the scale change results in some distortion (a line crossing the boundary other than normally changes direction) and also a slight change in signal level. All of these effects are corrected by the image processing software.

Each camera also shows  $\sim 5$  fault lines due to shear dislocations in the fibre-optic output faceplate of the UVC. The image on one side of a shear line may be displaced by a maximum of 50  $\mu\text{m}$  with respect to the other side. As these defects are highly localised and few in number, they can only interfere with data in a very few spectral elements.

There are also some intensity-dependent changes of image geometry; these are caused by "beam-pulling" effects in the readout section of the SEC tube (local charge variations on the SEC target produce electric fields which slightly deflect the read beam on its approach to the target). The magnitude of such image shifts can be of the order of 1 pixel between extremes of intensity. To reduce wavelength-determination errors due to this effect, it is necessary to use a reference spectrum (from the wavelength calibration lamp) exposed to approximately the same level in the spectral region of interest.

### 3.5 Background

In addition to a small contribution from the sky, there are several other sources of background (increase in output signal in the absence of input photons) intrinsic to the IUE camera system and its environment. These are considered below.

#### 3.5.1 Dark emission from the UVC and SEC photocathodes

Electrons from this source, mostly thermionic in origin, are indistinguishable from signal photoelectrons. The dark current from the  $\text{Cs}_2\text{Te}$  photocathode of the UVC at  $10^\circ\text{C}$  is typically  $1 \rightarrow 4$  electrons/ $\text{cm}^2$ /sec ( $1 \rightarrow 4 \times 10^{-5}$  electrons/pixel/sec) (Ref. 3-2), whilst that for the alkali photocathode of the SEC tube is typically 10 electrons/ $\text{cm}^2$ /sec. These result in a typical background signal of  $0.5 \rightarrow 1.5$  DN per hour's exposure, for a camera operating at SEC MAXG and with LO head-amplifier gain. Thermionic emission is temperature-dependent, and the background would be expected to decrease by a factor of 2 on reducing the environmental temperature from  $+10^\circ\text{C}$  to  $0^\circ\text{C}$ .

#### 3.5.2 Particle radiation

The radiation environment of the IUE orbit consists largely of electrons with a steeply decreasing spectrum in the energy range  $0 \rightarrow 3$  MeV. The radiation shielding ( $\sim 1\text{gm}/\text{cm}^2$  of aluminium) provided for the experiment cannot prevent the penetration of all particles, and the radiation which does penetrate to the cameras causes interference in the form of an increased background level. The magnitude of this background is strongly dependent upon orbital position because of the shape of the earth's radiation belts. Because of several uncertainties, accurate predictions of the radiation-induced background cannot be made, and the information given below is a best estimate from the data available. Detailed measurements of camera background as a function of orbital position will be made as part of the post-launch calibration of the IUE scientific instrument.

Experiments have shown that 90% of the background is due to the production of Cerenkov photons in the  $\text{MgF}_2$  faceplate of the camera, whilst the remaining 10% is due to direct stimulation of the P-11 phosphor in the UVC. The noise and uniformity of the background are similar to those obtained for an exposure to light producing the same mean output signal level.

The estimated background signal (expressed in DN per minute's exposure time at SEC MAXG) for the prime cameras as a function of orbital position is given in Fig. 3.5-1; for the redundant cameras, the background is expected to be less by some 40%. It can be seen that the radiation-induced background problem is most severe for two or three hours on either side of perigee and, in this region, observations may perhaps be limited to low dispersion or to comparatively bright objects at high dispersion.

### 3.5.3 Random bright spots

Long exposures usually show a number of small bright spots in the image. These occur randomly in time and in position in the image, and their incidence is typically 30 per hour's exposure. They originate in the UVC and are caused by radioactive disintegrations in the phosphor. The spots are often so bright as to produce a saturated output (especially when operating at SEC MAXG and with HI head-amplifier gain). Because they originate downstream of most of the resolution-degrading optical and electro-optical elements in the system, those spots which happen to fall within echelle orders may be readily distinguished from emission lines; the spot profiles are sharp and their full intensity is generally contained within two pixels.

### 3.5.4 UVC phosphorescence

In common with most fluorescent emitters, the P-11 phosphor in the UVC also exhibits phosphorescence, i.e. emission of light after the excitation (by UVC photoelectrons) has ceased. Under normal circumstances, the flood-lamp exposures during the PREPARE sequence are the most intense exposures experienced by the cameras, and the principal contribution to the phosphorescence component of background is the integrated effect of the phosphorescence arising from the PREPARE sequence; occasionally, one may also need to consider the phosphorescence arising from heavily over-exposed regions of the spectrum in a previous image.

Phosphorescence intensity ( $I_t$  - expressed as an equivalent photon input to the UVC) has a power-law dependence on time  $t$  after excitation, of the form:

$$I_t = k E t^{-n}$$

where  $k$  is a constant and  $E$  is the integrated intensity of the exciting exposure (exposure time assumed short compared with  $t$ ); the index  $n$  is typically  $\sim 0.75$ .

Measured values of n and k (for t in seconds) are as follows:

Camera	Slot	k	n
06	LWP	$1.2 \times 10^{-4}$	0.72
07	LWR	$2.9 \times 10^{-4}$	0.77
08	SWP	$1.8 \times 10^{-4}$	0.78
09	SWR	$1.0 \times 10^{-4}$	0.70

The magnitude of the effect is such that the phosphorescence from the PREPARE sequence will yield a signal of  $\sim 1$  DN in an hour's exposure at SEC MAXG (LO gain READ). A similar signal level would be obtained from a four-times over-exposed previous image; thus, in the case of very heavily over-exposed previous images, there may be significant contamination of the succeeding image.

Rate of increase of background (DN per minute)

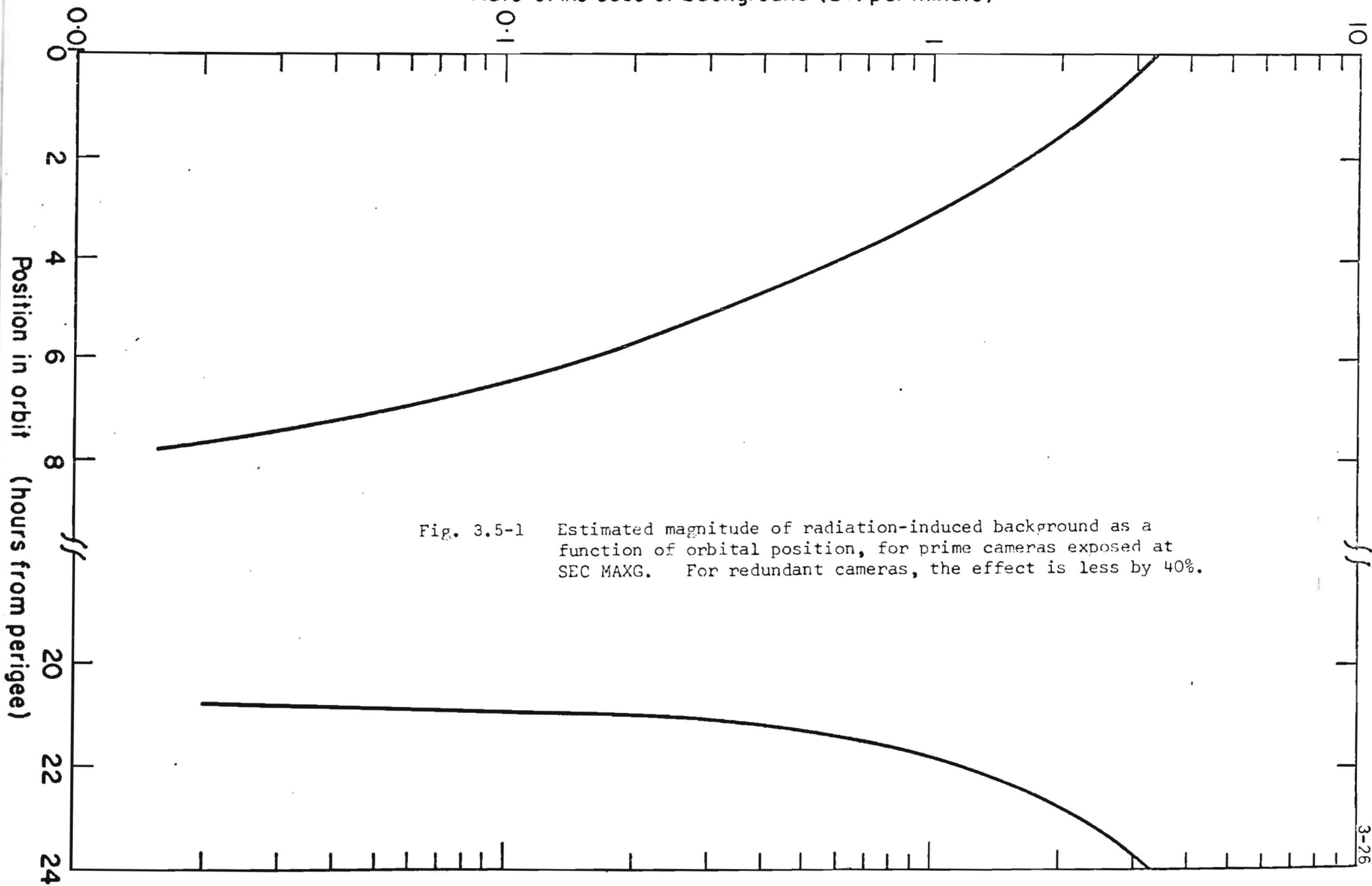


Fig. 3.5-1 Estimated magnitude of radiation-induced background as a function of orbital position, for prime cameras exposed at SEC MAXG. For redundant cameras, the effect is less by 40%.

### 3.6 Over-Exposure

A signal output of 205 DN in the LO head-amplifier gain mode is considered to constitute a full signal; at a target charge level of  $1.45 \times 10^5$  electrons per pixel, this corresponds to the onset of significant saturation of the ITF. The upper limit of the telemetry system is 255 DN, and no photometric information is available for regions of spectra which are over-exposed beyond this level.

In certain observing situations it will be necessary to over-expose parts of an image in order to study faint features in other areas of the spectrum. There are some limitations on this imposed by considerations of camera safety and of data integrity.

#### 3.6.1 Camera safety

The exposure level of the brightest part of the spectrum must not be allowed to exceed 1000 times that giving a full signal. Larger exposures may cause permanent damage to the SEC target.

#### 3.6.2 Data integrity

Data quality can be significantly affected by over-exposure in three different ways:

- (i) Halation effects. Halation (§3.3.0) causes image spread in the region of over-exposed features and an increase in the general background level of the image; this results in information loss (lower S/N) for faint spectral features.
- (ii) UVC phosphorescence (§3.5.4). A heavy over-exposure causes appreciable excitation of the UVC phosphor; the subsequent phosphorescence results in contamination of succeeding images.
- (iii) Residual images on SEC target. The normal PREPARE sequences (SPREP, LNPREP and FPREP - §2.4.4) adequately erase images up to moderate levels of over-exposure. Heavy over-exposures (greater than 00 x full signal but below the threshold for target damage) leave fairly persistent residual images on the SEC target; these normally decay away after several image operations. The SEC target recovery process can be greatly accelerated by the use of XPREP following the READ of a heavily over-exposed image, and preceding whichever PREPARE sequence is to be used for the next image.



### 3.7 Image Imperfections

Apart from the fiducial marks (§2.2), there are several other artefacts appearing on unprocessed IUE imagery; nearly all of them disappear after image processing (§5). Most of these have already been discussed, but for completeness they are all listed here together.

- (i) SEC target blemishes. These appear as small bright spots in the image. They are fixed in position, very sharply defined, and generally saturated in intensity (255 DN). There are less than five such blemishes on any of the cameras. Like fiducial marks, their only effect on data is to obscure a very small fraction of the image area. Another type of blemish is caused by local variations in target gain; this is removed in ITF correction (§5.5).
- (ii) Fibre-optic "chickenwire effect". A faint square mesh pattern is visible on flat field images. This is caused by the square bundle construction of the UVC's output fibre-optic window. It is completely removed by ITF correction (§5.5).
- (iii) Fault lines caused by dislocations in the UVC fibre-optic output (§3.4). These are not visible on flat field images, but only on spectra. As they are very localised, they do not interfere with data in more than one or two spectral elements (whose positions are known).
- (iv) Sensitivity steps at 115 and 250 pixels from the centre lines of the image (§3.4). Removed by ITF correction.
- (v) Random bright spots (§3.5.3). Readily identifiable.
- (vi) DAC error lines. Observed only when FPREP (the fast PREPARE sequence for quick-look images - §2.4.4) is used. The lines are slightly curved, approximately vertical, and arise from the inability of the deflection digital-to-analogue converters to cope with the fast scanning employed in this PREPARE sequence.

### 3.8 References

- 3-1. R A Powell, W E Spicer, G B Fisher and P Gregory, Phys. Rev. B. 8, 3987 (1973).
- 3-2. C I Coleman, Appl. Opt. 17, 0000 (1978)
- 3-3. A Boksenberg, in "Astronomical Observations with Television-Type Sensors", p. 311, Institute of Astronomy and Space Science, University of British Columbia, Vancouver (1973).
- 3-4. C I Coleman, Phot. Sci. Eng. 21, 49-59 (1977).

4. OPTIMUM USE OF CAMERAS

Efficient use of the IUE observatory requires advance preparation based on an understanding of the options available and their effects on data quality and observation time. The reasons for selection of several of these options will be clear whilst others will be less immediately obvious.

TN 31/1

#### 4.1 Available Options

The options available to the astronomer are listed below. (Note that there are certain additional commandable parameters which are adjusted infrequently by ground-station personnel only in order to 'tune-up' camera performance). Those options marked with an asterisk\* may only be exercised by a guest astronomer under special circumstances; normally, no variation from the standard settings will be permitted (note that even when non-standard options are permitted, the resulting operating modes will be uncalibrated).

- (i) \*Epoch of observation
- (ii) Spectrograph (long- or short-wavelength)
- (iii) Entrance aperture (small or large)
- (iv) Dispersion (HI or LO)
- (v) \*Camera (prime or redundant)
- (vi) Prepare sequence (SPREP, FPREP or LNPREP)
- (vii) SEC camera tube gain in EXPOSE (MAXG, MEDG or MING)
- (viii) Exposure time (and exposure meter option)
- (ix) Video head-amplifier gain in READ (HI or LO)
- (x) \*Pixel stepping interval (x1, x2, x3 or x4) in READ
- (xi) \*READ scan format (normally 768 x 768 pixels)

For some observations, the choice of settings will be fairly straightforward; thus, an observation of a very faint object may require the low-noise Prepare sequence (LNPREP) followed by exposure at SEC MAXG using the LO-dispersion mode of the spectrograph. For a bright source, where exposure time is not a problem, exposure at SEC MEDG will yield higher S/N, i.e. higher photometric accuracy. Most observations will, however, require that a compromise be made between sensitivity, S/N, dynamic range, etc. The dependence of these quantities on the several operating parameters is somewhat complicated. The basic performance characteristics of the IUE cameras have been described in §3. After more detailed consideration of the available options (§4.2 below), guidelines are given for selecting those most appropriate for a particular observational situation (§4.3).

4.2.1 Epoch of observation and scheduling

The UT (Universal Time) at which an observation is made will often be of no importance, and it is anticipated that only certain types of observation will require it to be specified (examples include occultations or exposures synchronised to a particular phase of a periodic variable). Scheduling such operations may present difficulties; in addition to the problem of accommodating the sometimes mutually exclusive wants of different guest observers, there are certain other restrictions. The most important of these are the satellite pointing constraints; these are dealt with in detail elsewhere (§00.00), but may be summarised as:

- (i) The satellite must not be pointed within  $45^\circ$  of the sun (normally, the satellite will be orientated with the tip of the telescope sunshade rolled towards the sun - this may impose an additional limitation on the position angle of the large spectrograph aperture in cases where it is desired to obtain information about spatial variations across an object). The principal sun-angle constraint is imposed by the upper limit on stray light entering the spectrograph; various other constraints (sun sensor, shading of solar arrays, thermal) must also be considered. It must be borne in mind that even at moderate sun-angles or earth-angles (see below), sky background/scattered light effects may be high enough to prevent the use of fainter guide stars. Targets in low ecliptic latitudes may not be observable for up to 90 days per year.
- (ii) The earth constraint depends upon the sun-earth relative angle and orbital position of the satellite. The earth constraint may vary in extent between  $\sim 50^\circ$  diameter and a full hemisphere.
- (iii) The minimum moon-angle is likely to be  $20$  to  $25^\circ$ ; as the moon moves  $\sim 13^\circ$  per day, this constraint (for a particular object) will only last for 3 to 4 days per month.

Computer programmes have been developed which take account of all the constraints, and display them for the whole sky and/or for a particular set of targets.

#### 4.2.2 Spectrograph

The choice of long- or short-wavelength spectrograph (wavelength ranges given in Table 1-1) will normally be clear cut. If it is only desired to examine spectral features in the overlap region of the two spectrographs, it may be preferable to select the short-wavelength spectrograph because of its higher optical efficiency and lower echelle order overlap in this region.

#### 4.2.3 Entrance aperture and dispersion

When working at HI dispersion, the small aperture will normally be used and the large aperture will be closed. When high spectral resolution is not required and/or when the object is too faint to give a usable signal in HI dispersion, the LO dispersion option will be selected. In LO dispersion, the system sensitivity is approximately 60 times increased (although obviously at correspondingly reduced spectral resolution). Because the telescope point spread function extends over more than 3 arc sec, the throughput of the system can be further increased by using the large entrance aperture (with a 'point' object, the signal/sky background ratio will decrease; with an extended object, some spatial information becomes available). Note that when the large aperture is used, the small aperture is also open; in this case, an extended object may yield two parallel spectra (one through each aperture).

#### 4.2.4 Camera

The general policy with regard to the use of prime and redundant cameras is to operate with only one of these and to avoid switching from one to another. Normally, calibration files will be held only for the camera in current use. In certain exceptional circumstances, the alternative camera might be used. Relevant considerations include:

- (i) Spectral features obscured by fiducial marks ( $\sim 1\%$  of the image area) on one camera will generally be observable using the alternative camera. The positions of fiducial marks (or target blemishes) are tabulated for each camera, and are indicated on spectral data plots.
- (ii) The redundant cameras are 40% less sensitive to radiation induced background (§3.5.2), and it may be advantageous to use the redundant cameras in high-radiation regions of the IUE orbit.
- (iii) In the short wavelength spectrograph, slightly higher optical transmission at short wavelengths ( $< 160$  nm) is achieved with the prime camera because of the absence of the camera select mirror.

#### 4.2.5 PREPARE sequence

In order to make the most efficient use of the IUE observatory, it is worthwhile to arrive at a compromise between photometric accuracy and observation time, depending upon the type of object being studied. A large part of the overhead time in obtaining an image is incurred by the PREPARE sequence. The standard sequence (SPREP) takes  $\sim 10$  minutes, and yields adequate S/N for the majority of spectra (see §3.2). Where the ultimate in small-signal detectability is required, the low-noise sequence (LNPREP) should be used. This results in an improvement in S/N for small signals of 00%, at the cost of an increase of  $\sim 5$  minutes in the overhead time; as exposures to faint objects will be long in any case, the increased overhead time will not be a serious penalty. It should be noted that detailed calibration data will not be available for imagery using LNPREP; however, provided that a null exposure (§3.1.2) using LNPREP is also available, photometric correction can be carried out with negligible error using the ITF calibrations applicable to SPREP.

Where image quality is of secondary importance, e.g. for exposure time determination or for verifying the presence of a particular spectral feature, the fast sequence (FPREP) may be used. This takes only  $\sim 3$  minutes; it provides good erasure of previous images but, because of the fast beam scanning method, leaves DAC error lines (§3.7) on the image. This is not a disadvantage for quick-look purposes, but means that accurate photometry cannot be carried out.

The use of XPREP after a heavily over-exposed image (and before any further image procedure) may be the responsibility of ground-station personnel.

#### 4.2.6 SEC camera tube gain

Both sensitivity (§3.1.2) and S/N (§3.2) of the cameras depend upon the SEC target gain in EXPOSE. At the upper setting (MAXG), a particular signal level may be reached in minimum time ( $\sim 1/3$  of that at MEDG, and  $1/10$  of that at MING); however, as may be seen from Fig. 3.2-1, the maximum S/N achievable at MAXG ( $S/N_{\max} \sim 35$  for a resolution element of  $3 \times 3$  pixels) is less than the ultimate attainable at MEDG with a longer exposure time ( $S/N_{\max} \sim 50$ ).

For very faint objects, where exposure levels of  $10^5$  photons per resolution element cannot be achieved in reasonable exposure times (up to  $\sim 1\frac{1}{2}$  hours), it is normally not worth going to MEDG and exposing for several hours to obtain the improved S/N. An important additional consideration here is the influence

or radiation-induced background (§3.5.2); as the noise in this will be effectively added to that of the wanted signal (thus reducing the ultimate achievable S/N), it will generally bias the choice of gain setting towards MAXG rather than MEDG.

Where the flux from spectral features of interest in the object exceeds  $\sim 10^5$  photons per resolution element in much less than an hour, it will generally be profitable to use the MEDG setting, thus giving higher ultimate S/N at optimum exposure and a somewhat larger dynamic range (Table 3.2-1) within which a particular S/N or photometric accuracy is achieved.

At MING, the S/N performance as a function of input signal is slightly worse than at MEDG. However, MING is useful for very bright objects (flux greater than  $\sim 10^4$  photons per resolution element per second - requiring only a few seconds exposure at MAXG) as they can be given a longer, and therefore several times more accurate, exposure time than at MEDG or MAXG.

It should be noted that halation is slightly less at the lower gain settings (i.e. the wings of the PSF are reduced in intensity) although the PSF core is slightly increased in size; this consideration may be of importance for sensitive measurements of equivalent width.

#### 4.2.7 Exposure time

The duration of an exposure may be commanded from zero upwards as an integral number of seconds, or in minutes and seconds. The longest useful exposure time, in the region of several hours, is set by the maximum tolerable background level (radiation-induced, scattered light, etc.) and by scheduling and pointing constraints. As pointed out in §2.4.2, it is inadvisable to use short exposures (<25s) for photometry accurate to better than 2%, because of the uncertainty in exposure time of  $\lesssim 0.5$ s due to the finite rise- and fall-times of the camera EHT supplies. Whilst this uncertainty can, in principle, be absolutely calibrated, there is a second effect to be considered; there is also a very slight change of focus and image scale when the EHTs are changing. Thus, it will normally be necessary to choose a lower SEC gain setting with a correspondingly increased exposure time. It is possible that other techniques for shuttering short exposures may be developed; these include (i) using the sun shutter and (ii) drifting the star at a controlled rate across the spectrograph entrance aperture.



The exposure time must obviously be chosen so that spectral features of interest are neither driven into saturation (approaching or exceeding the 255 DN limit nor of such low signal level as to yield inadequate S/N. Over-exposure must always be guarded against (see WARNING in §3.6.1).

For maximum photometric accuracy, the exposure time should be chosen (using Figs. 3.3-3 and 3.3-4) so that the desired parts of the spectrum reach as nearly as possible the level at which optimum S/N is achieved. In practice, it will be necessary to use a compromise value to accommodate the range of intensities of the different spectral features; it must also be remembered that the sensitivity and S/N performance of the cameras and the efficiency of the spectrograph are all functions of image position/wavelength. It may frequently prove necessary to obtain more than one image for adequate exposure of different parts of the spectrum.

Where it is not possible to make a reasonable estimate of exposure time based on prior knowledge of the object under study, it will often be useful to obtain a trial image using the fast PREPARE sequence (FPREP). For most objects, the trial exposure will typically be of a few minutes duration at SEC MAXG, followed by a LO-gain READ; for bright objects, however, trial exposures should be shorter and should be made at MING to avoid any risk of over-exposure. The resulting trial image will then be examined using the EDS (§6.1.1) and the correct exposure time calculated from the signal level of the features of interest. (Note that for signal levels up to  $\sim 150 \rightarrow 200$  DN, it will be sufficiently accurate to assume that the ITF (§3.1.2) is linear. It is important to remember that the signal level obtained from the raw image using the EDS is superimposed on the null level ( $\sim 20$  DN, depending upon camera and position in the image); this must be taken into account when computing an exposure time from the results of a trial exposure.)

The effective exposure time depends upon the guidance accuracy of the IUE telescope, especially when the small spectrograph aperture is in use. An optional 'exposure meter' facility (COMPX) has been designed which (using the OBC) compensates the exposure time for any time during which FES data show that the star has drifted out of the entrance aperture. Use of this option is described elsewhere (§00.00).

#### 4.2.8 Head-amplifier gain

The HI head-amplifier gain setting yields a three times smaller digitisation error for signal levels up to one third of the LO-gain full-scale. As digitisation noise is only one component of the total system noise, the improvement in S/N for small signals using HI gain is fairly small (see Fig. 3.2-1). If the signal level (including the null level) from a very faint source is unlikely to exceed 85 DN in LO gain, there will be some advantage in going to HI gain. In most cases, however, it will be preferable to expose to a higher signal level in order to maximise the S/N, and then LO gain must be selected.

#### 4.2.9 Pixel size, scan format and telemetry rate

The pixel size, or pixel stepping interval, is normally set at  $\times 1$  (i.e. 37  $\mu\text{m}$  referred to the camera input). The READ beam can also be stepped at 2, 3 or 4 times this interval in both sample and line directions with a corresponding saving in scan time. Whilst this facility is of use for certain camera testing work, it is unlikely to be required for observations of spectra because (i) resolution is reduced, (ii) the physical size of the read beam is such that not all the charge in the enlarged pixel can be read out, (iii) the ITF shape is completely changed and the mode is therefore uncalibrated.

The standard READ scan format is a square 768  $\times$  768 pixel raster which completely over-scans the circular SEC target. It is possible to read out only a smaller rectangular area at more or less any position on the target. This may, however, be a hazardous operation and there is no real advantage in performing a partial READ except a possible small saving in scan time when it is required to examine only one small portion of the spectrum. Note also that there will be edge effects which will result in inaccurate data at distances of up to  $\sim 5$  pixels from the edges of a reduced scan format.

The pixel stepping rate during PREPARE and READ is locked to the telemetry rate and therefore, in order to minimise operation times, the fastest rate available (40 kbs) will generally be used. This will certainly apply for all PREPARE sequences, and for all READs of images when highly accurate photometry is not essential. As the analogue-to-digital conversion accuracy for the video data is slightly degraded at the 40 kbs rate, it may be worthwhile to switch to 20 kbs when particularly high quality data are required.

#### 4.3 Classes of Observation and Setting of Operational Parameters

From the preceding section (§4.2), it should already be fairly clear how to determine the correct operating parameters for a given observation. The choice of spectrograph (§4.2.2) should be made first. Table 4.3-1 summarises the principal categories of observation, their requirements in terms of system performance, and the operational parameters which should be selected accordingly. Determination of the correct exposure time then follows as in §4.2.7.

Table 4.3-1

Classes of Observation and Settings of Operational Parameters

Class of observation	Performance requirements	Operational settings
1. Accurate measurement of strong sources.	Maximum S/N and dynamic range. High spectral resolution.	SPREP, SEC MEDG, READ LO. Short exposure time. (Use MING if the object is very bright). Use small entrance aperture, unless absolute photometry required.
2. Accurate measurement of medium-strength sources.	As above	SPREP, SEC MEDG, READ LO. Exposure time may be long, and MAXG will then be preferable.
3. General measurement of medium-strength sources.	As above, but slightly reduced S/N acceptable.	SPREP, SEC MAXG, READ LO.
4. Detection of weak sources at high dispersion.	Maximise S/N for small signals. Minimise background.	LNPREP, SEC MAXG, READ LO. Long exposure time. (Use READ HI if 85 DN level will not be reached with long exposure and READ LO). Avoid part of orbit within 2 or 3 hours of perigee.
5. Measurement of weak (e.g. extragalactic) sources.	Low spectral resolution and increased sensitivity. Adequate S/N.	LO dispersion. SPREP, SEC MAXG, READ LO. Long exposure time.
6. Detection of sources at limit of IUE sensitivity.	Low spectral resolution and increased sensitivity. Maximise S/N for small signals. Minimise background.	LO dispersion. LNPREP, SEC MAXG, READ LO. Long exposure time. LO dispersion. (Use READ HI if 85 DN level will not be reached with long exposure and READ LO). Avoid part of orbit within 3 hours of perigee.
7. Trial image to determine correct exposure time.	Minimise time.	FPREP, SEC MAXG, READ LO. Few minutes' exposure. (MING and short exposure if object known to be bright).

#### 4.4 Calibration Images

For many types of observation, the guest astronomer will not need to obtain any additional calibration images, as the ITF calibrations for the two cameras in current use will be regularly updated by IUE project staff. When non-standard camera settings are used, or when there are special requirements on the accuracy of image data extraction, the astronomer may need to take additional images (the additional time required for obtaining these extra images must not be forgotten).

Examples of additional data which might be required include:

- (i) For improved accuracy wavelength determination: wavelength-calibration lamp images exposed to the same level as the stellar feature being measured (this may also require the spacecraft to be at the same attitude relative to the sun because of thermal considerations.
- (ii) For more accurate geometric correction: a flat field image (using UV floodlamp) exposed with the spacecraft at the same sun-angle.
- (iii) For improved photometry (perhaps depending on length of time since last calibration, or with non-standard settings): a null and one or more flat-field images; stellar standard(s).

## 5. IMAGE PROCESSING SOFTWARE

The IUE cameras depart significantly from the ideal of uniform, linear, distortion-free, photon-noise-limited detectors. The main points to be considered, as discussed in §3, are:

- (i) Geometrical distortion.
- (ii) Non-linear and non-uniform photometric response.
- (iii) Resolution degradation.
- (iv) Image imperfections, periodic noise, particle radiation background.
- (v) Wavelength-dependent variations in transmission of optics and camera sensitivity.

In order to produce accurate measurements of ultraviolet flux as a function of wavelength, it is necessary to carry out several sequential image processing operations. A block diagram of the IUE Spectral Image Processing System (IUESIPS) is shown in Fig. 5-1.

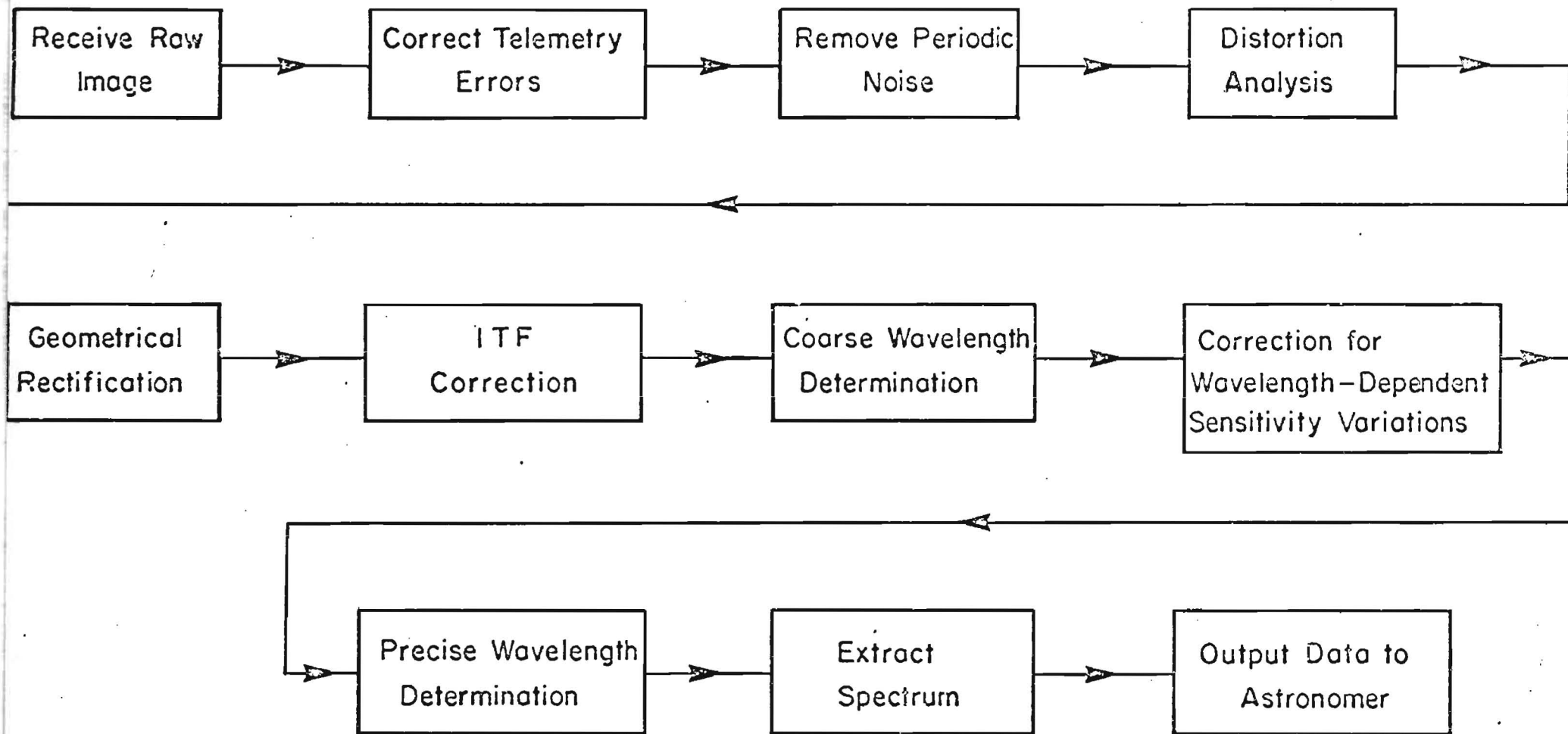


Fig. 5-1 Block diagram of the IUE Spectral Image Processing System (IUESIPS).

The software system IUESIPS is based on the Jet Propulsion Laboratory's VICAR system and has been developed at GSFC and at the Appleton Laboratory (Ref. 5-1). IUESIPS runs in parallel with, but is quite separate from, the spacecraft control computer system.

Images of maximum size 768\*768 pixels are telemetered from the satellite and stored on disc at the ground station. The signal is digitised to 8-bit accuracy; each pixel is thus represented by a data number (DN) between 0 and 255. IUESIPS is used to execute a number of software tasks on the stored data by calling a sequence of image processing programs. This is done in a high level image processing language (VTRAN) which normally requires only one line of text per program call. The system is interactive, so intermediate results can be checked before proceeding and, if necessary, changes can be made. The following is an example of the construction of a processing task which applies geometric and photometric correction to an image and then plots the result:

```
E, GEOM, IN, A, (1, 1, 768, 768), GPARAM
```

```
E, FICOR, A, B, (1, 1, 768, 768), FPARAM
```

```
E, IUEPLOT, B, *, (1, 1, 768, 768), PLOT
```

Here, E denotes the execution of the programs GEOM, FICOR and IUEPLOT. IN is the initial image, A is an intermediate and B is the final image. The size of each input image is given in parentheses and this is followed by the parameters required for each program, e.g. fiducial mark positions in GPARAM and the name of the ITF table in FPARAM. If the plot shows image B to be properly corrected, it will be used for further software processing, e.g. extraction of echelle orders. In a complete processing task, extra operations are, of course, required for such purposes as accessing calibration files or writing the final corrected spectrum on tape.



## 5.2 Removal of Telemetry Errors

Dislocations in an image are caused by occasional telemetry dropouts (missing minor frames of data). Software schemes piece together the valid minor frames of data in their correct image positions.

### 5.3 Periodic Noise Removal

In order to remove periodic noise, the down-link data stream must first be reconstructed in time, by making allowance for the fact that the image is transmitted as 48 pixels of image information alternating with 16 words of spacecraft engineering data. After the data stream has been temporally reconstructed, it is Fourier transformed and a power spectrum is obtained. The noise frequencies are identified by inspection of the power spectrum and are removed from the transformed data. Finally, an inverse transform is taken and the gaps containing the spacecraft data are closed. The resultant image is free from periodic noise.

Geometrical distortion in the IUE images is measured by reference to the fiducial marks (§2.2 and Fig. 2.2-2). These are located by the programs to an accuracy of at least 0.5 pixel, and usually two or three times better in a flat-field image. Correction for fixed-pattern noise, with significant pixel-to-pixel variations, requires a positional accuracy of at least 0.5 pixel in the distortion measurement; a geometrical error of one pixel is sufficient to reduce S/N by a factor of  $\sqrt{2}$  in the photometrically corrected image.

The fiducial marks are located using a matrix correlation technique. The measured positions are fitted by third degree polynomials using a least squares method. Along a line in the image there are between 8 and 13 fiducial marks, while only four are needed for the determination of a polynomial. This redundancy is used to improve the accuracy of the fiducial mark position determination and/or to fill in the positions of 'missing' fiducial marks. In spectral images, it is sometimes difficult to locate a sufficient number of fiducial marks for geometric correction; an observer may then need to obtain a flat field image (using the UV flood-lamp) under identical circumstances and at the same mean exposure level as the spectrum. The set of fiducial mark positions determined from the flat field then defines the geometry of the spectrum.

Once the positions of the marks in the distorted image are known, the image is geometrically corrected using a piecewise bilinear transformation which brings the observed fiducial marks back onto a perfectly square grid. This procedure is carried out at an early stage of image processing, so that spectra and calibration tables are brought to a common frame of reference.

## 5.5 Photometric Correction

The response of the IUE cameras is non-linear and the sensitivity is dependent upon position in the image (§3.1.2). Because of the presence of small-scale fixed-pattern noise, photometric correction must be done on a pixel-by-pixel basis. As the UVC is linear over many orders of magnitude, it is possible to separate the flux-dependent and the wavelength-dependent parts of the photometric correction process. Photometric correction converts the measured signal at each pixel to equivalent flux at 253.7 nm incident on the camera, by interpolation (linear or quadratic) in the intensity transfer function (ITF) tables. The system sensitivity correction (§5.13 below) completes the operation by applying the wavelength dependent part of the correction (for UVC quantum efficiency and spectrograph optical efficiency).

The ITF tables contain about 10 points per pixel or  $\sim 6 \times 10^6$  bytes per table. As compilation, construction and storage of ITF tables is a considerable burden on the available facilities, only six tables are regularly updated and available for standard data processing. These six tables comprise three each (at the SEC MAXG, MEDG and MING settings) for a single short-wavelength camera and a single long-wavelength camera; they apply only for use with SPREP and LO gain in READ (for READ in HI gain, ITF correction may be carried out using a factor of 3 to correct for the increased head-amplifier gain). The ITF tables are not valid for images taken with FPREP or LNPREP, although they will not be too inaccurate with the latter.

Each data point in an ITF table is built up from  $n$  images; the random noise in the table is thus  $n^{1/2}$  times the random noise in a single flat field image (§3.2).

The spectra of the high priority targets, the first IUE observations, will be analysed using the ground-based calibration data. Later, the ITF calibrations will be up-dated using exposures to the on-board UV floodlamps.

5.0 background removal

Unwanted background contributions, originating in the cameras or radiation-induced, are removed using calibration images taken under appropriate circumstances.

Most image imperfections (§3.7) (e.g. the sensitivity steps occurring at 115 and 250 pixels from the image centre, shading, fibre-optic "chicken-wire" effect) disappear after photometric correction.

There exists a program for removal of fiducial marks from flat field images; however, it is not used for removing fiducial marks from spectra.

At present, no restoration of resolution through software techniques is planned. Typical point spread functions are available to the astronomer (see also §3.3).

The program WAVECAL is applied to a calibration spectrum from the Wavelength Calibration lamp, in order to derive precise dispersion constants. These latter are used for wavelength determination in spectral images.



#### 5.10 Extraction of Spectra from Corrected Images

Spectral intensity determination is carried out using a program (DATEXT) which calculates the integrated intensity in a pseudo-slit which is passed along each echelle order, thereby creating a table of  $I(\lambda)$ . Additional programmes sort the data and produce a plot of  $I$  vs.  $\lambda$ .

The I vs.  $\lambda$  data can be corrected for order overlap/scattered light using measurements of the inter-order intensity. The correction requires that the spectral intensity data be re-arranged in their original two-dimensional echelle format.

## 5.12 Sky Background Removal

This is carried out in the same way as background removal, using a sky-background calibration image.

### 5.13 System Sensitivity Correction

The calculated fluxes are corrected for the wavelength-dependent components of the system sensitivity (optical efficiency and camera quantum efficiency). The system sensitivity is determined using stellar standards for which absolutely calibrated spectra exist. (Initially, system sensitivity data will be derived from ground-based measurements.)

5-1. D A KlingleSmith and E Dunford, in "Image Processing Techniques in Astronomy", Reidel, Dordrecht, pp 135-139 (1975).

## 6. GROUND STATION DISPLAY FACILITIES

### 6.1 Image Display

#### 6.1.1 The IUE Experiment Display System (EDS)

The EDS contains a colour cathode ray tube (CRT) controlled by a mini-computer. Two complete images may be stored on disc, and either one of them may be displayed in black-and-white or in false colour on the CRT. A joystick-controlled cursor may be used to specify image coordinates to the computer. The capabilities of the EDS include:

- (i) Display one of two stored images.
- (ii) Display histogram of DN values of a full or partial image.
- (iii) Change the intensity transfer function in any of eight different ways (e.g. CRT brightness proportional to intensity or log intensity, look at low-intensity features on expanded scale).
- (iv) Alter the pseudocolour representation of DN values.
- (v) Display an intensity plot of DN values along a line between any two points in the image.
- (vi) Expand portions of an image up to nine times.
- (vii) Translate portions of an image in both x and y.

#### 6.1.2 Photowrite

The Optronics Photowrite system is used to produce photographic film images from data stored on magnetic tape. The digital signals from the tape are converted to an analogue current; this modulates the brightness of a light emitting diode which is raster scanned relative to the film. Films are processed automatically and photometric reproducibility from one film to another is very good. Dimensional accuracy is excellent; the image scale is usually 100  $\mu\text{m}$  or 200  $\mu\text{m}$  per pixel.

Control of the IUE Scientific Instrument (SI) is exercised from a keyboard and CRT screen at the ground station. A procedure name with appropriate arguments is typed in at the keyboard to initiate and carry out the required camera operation. The statements of the procedure generate the appropriate spacecraft commands in the correct order and with the correct timing to set camera voltage levels, SI mechanisms, telemetry format, lamps, etc., safely as required. The camera control function is complex and requires simultaneous monitoring of many channels of information. A compact display has been developed for this purpose.

The Camera Operational Display fills a CRT screen and is divided into six sections:

- (i) CRT Header and Procedure execution status (2 lines) (PROC)
- (ii) Status of the Scientific Instrument (7 lines) (SISTAT)
- (iii) Out of limits display for the four cameras (6 lines) (MLIMSTAT)
- (iv) The status of the camera being currently commanded (4 lines) (CAMSTAT)
- (v) Last keyboard entry line. (1 line)

(i) The header serves to provide the computer system status (idle or active) and UT. The procedure execution status is given by the name of the procedure being used and the last statement in this procedure that was executed; this is updated every four seconds and shows the progression through a procedure. A telemetry frame counter shows data is being received by the ground station.

(ii) The scientific instrument status section includes:

current image number for each camera,  
power and operational mode status for each camera,  
status of all lamps and spectrograph and camera calibration,  
status of mechanisms relating to choice of dispersion (HI/LO),  
camera (prime/redundant) and aperture (large aperture open/closed),  
Fine Error Sensor operating mode.

An important piece of information relating to cameras is the time remaining in EXPOSE or READ mode. This is essential for the timely initialisation of the procedures required in carrying out a sequence of exposures and observations.

The choice of spectrograph is not displayed as this is decided by which spectrograph entrance aperture the star is manoeuvred to.

(iii) The out of limit section displays the camera parameters being checked and whether each parameter is above, within or below limits. Each parameter is identified by a position in one of the lines of the table. This position can hold one of four characters (\* \* H L) signifying

- \* - limit is not being checked
- \* - limit is being checked and is within limits
- H - limit is being checked and is above higher limit
- L - limit is being checked and is below the lower limit.

In the event of any H's or L's appearing in the display, other CRT displays will be used to identify and determine the value of the out of limits parameter. There may also be an audible alarm generated when any parameter goes out of limits.

(iv) This section contains housekeeping data for the camera under current procedure control. It displays the camera operating voltages and currents in engineering units, and the commanded and telemetered scan parameters.

(v) This line is entered by the observer and is for his comments.



CEM	Camera Electronics Module
CHM	Camera Head Module
CRT	Cathode Ray Tube
CSIM	Camera Supply Interface Module
DAC	Digital to Analogue Converter
DN	Data Number (digitised output signal of camera)
EDS	Experiment Display System
EEA	Experiment Electronics Assembly
EHT	Extra High Tension (voltages > 1kV)
FES	Fine Error Sensor
FWHM	Full Width at Half Maximum
GSFC	Goddard Space Flight Center
ITF	Intensity Transfer Function
IUE	International Ultraviolet Explorer
IUESIPS	IUE Spectral Image Processing System
LWL	Long Wavelength
LWP	Long Wavelength Prime camera
LWR	Long Wavelength Redundant camera
MAXG	Maximum gain setting of the SEC tube
MEDG	Medium gain setting of the SEC tube
MING	Minimum gain setting of the SEC tube
MTF	Modulation Transfer Function
OBC	On-Board Computer
PSF	Point Spread Function
QE	Quantum Efficiency
RMS	Root Mean Square
SCL	Scan Control Logic
SEC	Secondary Electron Conduction television camera tube (or, more specifically, its target)
S/N	Signal-to-RMS noise ratio
SWL	Short Wavelength
SWP	Short Wavelength Prime camera
SWR	Short Wavelength Redundant camera
UCL	University College London
UT	Universal Time
UV	Ultraviolet
UVC	Ultraviolet-to-Visible image Converter
VICAR	Video Image Communication and Retrieval image processing system
VILSPA	Villafranca del Castillo, Spain (IUE European ground station)

## Meeting Support

coffee donuts for 2 days, 30 people. \$180

P.M. coffee, soda, fruit " " \$150